FABRICATION OF POLYMER-BASED GAS SENSOR FOR VOLATILE ORGANIC COMPOUND GASES SENSING

NOOR ATHIRAH BINTI MUHAMMAD ‘AZMI

UNIVERSITI TEKNIKAL MALAYSIA MELAKA

FABRICATION OF POLYMER–BASED GAS SENSOR FOR VOLATILE ORGANIC COMPOUND GASES SENSING

NOOR ATHIRAH BINTI MUHAMMAD ‘AZMI

This report is submitted in partial fulfilment of the requirements for the degree of Bachelor of Electronic Engineering with Honours

Faculty of Electronics and Computer Technology and Engineering
Universiti Teknikal Malaysia Melaka

2024

UNIVERSITI TEKNIKAL MALAYSIA MELAKA
FAKULTI TEKNOLOGI DAN KEJUTERAAN ELEKTRONIK DAN KEJURUTERAAN KOMPUTER

BORANG PENGESAHAN STATUS LAPORAN
PROJEK SARJANA MUDA II

Tajuk Projek : Fabrication of Polymer–Based Gas Sensor for Volatile Organic Compound Gases Sensing

Sesi Pengajian : 2023/2024

Saya NOOR ATHIRAH BINTI MUHAMMAD ‘AZMI mengaku membenarkan laporan Projek Sarjana Muda ini disimpan di Perpustakaan dengan syarat-syarat kegunaan seperti berikut:

1. Laporan adalah hakmilik Universiti Teknikal Malaysia Melaka.
2. Perpustakaan dibenarkan membuat salinan untuk tujuan pengajian sahaja
3. Perpustakaan dibenarkan membuat salinan laporan ini sebagai bahan pertukaran antara institusi pengajian tinggi.
4. Sila tandakan (✓):

☐ **SULIT*** (Mengandungi maklumat yang berdarjah keselamatan atau kepentingan Malaysia seperti yang termaktub di dalam AKTA RAHSIA RASMI 1972)

☐ **TERHAD*** (Mengandungi maklumat terhad yang telah ditentukan oleh organisasi/badan di mana penyelidikan dijalankan.

☑ **TIDAK TERHAD**

Disahkan oleh:

(TANDATANGAN PENULIS)

(COP DAN TANDATANGAN PENYELIA)

Alamat Tetap: NO 280,
PEKAN KUAK,
33400,
LENGGONG,
PERAK.

TS. DR. SITI AMANIAH BINTI MOHD CHACHULI
Pensyarah Kanan
Fakulti Teknologi dan Kejuruteraan Elektronik dan Komputer
Universiti Teknikal Malaysia Melaka

Tarikh : January 2024

Tarikh : January 2024

*CATATAN: Jika laporan ini SULIT atau TERHAD, sila lampirkan surat daripada pihak berkuasa/organisasi berkenaan dengan menyatakan sekali tempoh laporan ini perlu dikelaskan sebagai SULIT atau TERHAD.

DECLARATION

I declare that this report entitled “FABRICATION OF POLYMER–BASED GAS SENSOR FOR VOLATILE ORGANIC COMPOUND GASES SENSING” is the result of my own work except for quotes as cited in the references.

Signature : ……………………………………………..

Author : Noor Athirah binti Muhammad ‘Azmi

Date : January 2024

APPROVAL

I hereby declare that I have read this thesis and in my opinion, this thesis is sufficient in terms of scope and quality for the award of Bachelor of Electronic Engineering with Honours.

Signature : ……………………………………………

Supervisor Name : Dr Siti Amaniah binti Mohd Chachuli

Date : January 2024

DEDICATION

This project is dedicated to my honourable supervisor, Dr. Siti Amaniah binti Mohd Chachuli, my respectable parents, and my fellow friends. All of them are always dear and near to me, and without their patience, care, understanding, unsparing support, affection, and, most of all, most profound love, it would not have been possible to come up with this project and thesis. It is a prayer to Allah that gives success and prosperity to everyone who helped me with the project.

ABSTRACT

Detecting VOC gases such as ethanol and acetone is a critical concern for public health and environmental safety, as prolonged exposure to ethanol vapour at the explosive limit volume of roughly 3.3% - 19% can cause nausea, skin rashes, and Parkinson's disease. In contrast, exposure to acetone vapor can lead to symptoms like bronchitis, weariness, and organ damage. Therefore, a device such as a gas sensor is needed to detect the VOC gases. This project aims to develop a polymer-based gas sensor for volatile organic compounds and to analyse the characteristics of the sensor in terms of response, response time, and recovery time. This project used graphene as the sensing material, chitosan as the polymer, and Kapton as the substrate. Initially, the interdigitated electrode was deposited onto the substrates using screen-printing and annealed at 150 ^{o}C for 10 minutes. Afterward, the graphene paste was deposited on the electrode using the doctor blade and annealed at 150 ^{o}C for 30 minutes. SEM and Raman characterizations are carried out to verify the sensing material of the gas sensor. The results revealed that gas sensors prepared by paste B (T2-1, T2-2) exhibited better response to acetone and ethanol than paste A (T1-1, T1-2), with response values of 1.0703 and 1.1389, respectively. The faster response time towards acetone is T2-1-

S3(2) (3 minutes), while in ethanol, it is T2-2-S1(1) (17 minutes). In conclusion, the polymer-based gas sensor produced better response toward acetone compared to ethanol.

ABSTRAK

Pengesanan gas VOC seperti etanol dan asetona adalah suatu aspek yang penting untuk kesihatan awam dan keselamatan alam sekitar, kerana pendedahan yang berpanjangan kepada gas etanol pada kadar bahaya sekitar 3.3% - 19% boleh menyebabkan mual, ruam kulit, dan penyakit Parkinson. Sebaliknya, pendedahan kepada gas asetona boleh menyebabkan gejala seperti bronkitis, keletihan, dan kerosakan organ. Oleh itu, alat pengesan gas diperlukan untuk mengesan gas VOC ini. Projek ini bertujuan untuk mencipta sensor gas berasaskan polimer untuk sebatian organik volatil dan menganalisis ciri-ciri sensor dari segi tindak balas, masa tindak balas, dan masa pemulihan. Projek ini menggunakan grafin sebagai bahan pendeteksian, kitosan sebagai polimer, dan Kapton sebagai substrat. Pada awalnya, elektrod berinterdigitasi dilapik ke atas substrat menggunakan cetakan skrin dan dibakar pada suhu 150 ºC selama 10 minit. Selepas itu, sebatian grafin dilapik pada elektrod menggunakan doctor blade dan dibakar pada suhu 150 ºC selama 30 minit. Karakterisasi SEM dan Raman dijalankan untuk mengesahkan sifat sebatian grafen yang dihasilkan. Hasil kajian menunjukkan bahawa alat pengesan gas yang disediakan oleh sebatian B (T2-1, T2-2) menunjukkan tindak balas yang lebih baik terhadap asetona dan etanol berbanding sebatian A (T1-1, T1-2), dengan nilai tindak balas masing-masing 1.0703 dan 1.1389. Masa tindak balas yang lebih cepat terhadap *asetona adalah T2-1-S3(2) (3 minit), manakala terhadap etanol, ia adalah T2-2-S1(1) (17 minit). Kesimpulannya, alat pengesan gas berasaskan polimer memberikan tindak balas yang lebih baik terhadap asetona berbanding etanol.*

ACKNOWLEDGEMENTS

In Allah's Name, The Most Gracious and Merciful

All praise to Allah and his blessing that this project may be completed. I thank God for the opportunities, trials, and abilities I had to finish writing this thesis. I had so much experience during this process, not just from the academic and personality sides. My humblest gratitude goes to the holy Prophet Muhammad (Peace be upon him), whose way of life has been a continuous guide for me.

First, I would like to sincerely thank my supervisor, Dr. Siti Amaniah binti Mohd Chachuli. She has given direction, understanding, courage, and, most importantly, positive encouragement and a warm soul to complete this project. It was a terrific pleasure and honour to have her overseeing me.

My deepest thanks go to my respectable parents for their support and attention, who inspired me to go my way. I would only be able to complete this thesis with their support. Special thanks go to my colleagues who helped me complete the thesis, they all exchanged exciting ideas and thoughts and made it possible to complete my project with accurate information. May God shower the above-cited personalities with success and honour in their life.

TABLE OF CONTENTS

LIST OF FIGURES

LIST OF TABLES

LIST OF SYMBOLS AND ABBREVIATIONS

VOC : Volatile organic compound

ppd : Purified protein derivative

rGO : Reduced graphene oxide

CNT : Carbon nanotube

SEM : Scanning electron microscopy

XRD : X-ray diffractometry

CS : Chitosan

GO : Graphene oxide

PSC : Perovskite solar cell

OSC : Organic solar cell

DSSC : Dye-sensitized solar cell

P3HT : Poly(3-hexylthiophene)

2D : Two-dimensional

PEDOT : Poly(3,4-ethylenedioxythiophene)

MWCNT : Multi-walled carbon nanotubes

SWCNT : Single-walled carbon nanotubes

NH_3 : Ammonia

NO_2 : Nitrogen dioxide

UV	:	Ultraviolet
PANI	:	Polyaniline
SnO_2	:	Tin(IV) oxide
R_a	:	Resistance in dry air
R_g	:	Electrical resistance
τ_{res}	:	Response time
τ_{rec}	:	Recovery time

LIST OF APPENDICES

CHAPTER 1

INTRODUCTION

1.1 General Overview

The current lifestyle relies heavily on many items containing volatile organic compounds (VOCs), which are unavoidable due to their pleasing performances and applications [1]. Volatile organic compounds (VOCs) are colourless gases that certain liquids or solids release. VOC gas encompasses a vast range of natural and artificial chemical compounds. Acetone, acetic acid, acetylene, benzene, ethanol, formic acid, methanol, isopropanol, and toluene are examples of common VOC gases. VOC emissions are emitted by building materials (such as carpet, paint, and composite wood products), personal care things (such as cosmetics, nail removers, and hand sanitisers), and everyday household items (such as cooking gas, fuel oil, and dry cleaning).

Volatile organic compounds (VOC) are flammable gases, so it is easy to cause combustion when exposed to high temperatures.

Furthermore, VOC gas will have an impact on human health. According to the Minnesota Department of Health, exposure to high amounts of VOC gas in the short term (hours to days) can cause headaches, dizziness, worsening asthma symptoms, vomiting, and eye, nose, and throat irritation [2]. While VOC gas has a high percentage of chronic exposure (years to a lifetime), humans may experience symptoms such as cancer, central nervous system damage, and liver and kidney damage [2].

Ethanol and acetone are two examples of volatile organic compounds (VOCs) that are ubiquitous daily because of their application in many industries. Ethanol produces most chemicals, foods, and pharmaceuticals [3]. Acetone is also used in the manufacture of most cosmetics and pharmaceuticals. It also shares characteristics with VOC gases, which are colourless, explosive, and can harm human and animal health. According to the research, ethanol has various adverse effects, including carcinogenicity, toxicity, skin irritation, and liver damage. In addition, several drunk-driving accidents have also been reported. As a result, ethanol is regarded as a poisonous and harmful gas, and ethanol monitoring is critical for living and working settings [4]. According to previous research, the acetone concentration in healthy people's exhaled breath ranges from 200 to 900 ppm [5]. Furthermore, acetone is a contaminant that enters the environment through landfill leachates, emissions from chemicals and other industries, automobile exhaust, and emissions. Acetone has also been found as a biomarker for diabetes. Currently, non-invasive methods for illness monitoring, such as gas sensors, are frequently employed [6].

A gas sensor is required to detect and identify this type of gas. Even though numerous commercially available gas sensor devices exist, there still needs to be more reliability, sensitivity, and accurate environmental monitoring. Abu-Hani et al. [7] noted that most currently available sensors suffer from drawbacks such as high cost, power consumption, poor stability, inflexibility, and malfunction in harsh environments. In recent years, polymers have gained significant attention for the fabrication and development of gas sensors due to their potential applications. Previous research has demonstrated several advantages of polymers, including ease of synthesis, operation at room temperature, fast response time, and high sensitivity to various gases, making them a promising material for gas-sensing applications [8]. Therefore, this study focuses on fabricating a gas sensor based on polymer to detect ethanol and acetone gases.

A gas sensor is an analyser that responds to a particular analyte selectively and irreversibly and translates input chemical quantities, such as the concentration of a single sample component or an entire composition analysis, into an electrical signal. Cu1-xZnxO [9], indium (III) sulfide [10], graphene [11], reduced graphene oxide [12], nickel oxide [13], zinc oxide [14], cerium (IV) oxide [15], agarose [16] and tin oxide [15] are some sensing materials for gas sensors that have been developed to detect acetone and ethanol gas. Graphene is widely used because of its large surface area of 2630 m2/g and high conductivity of 2.11 S/m[11]. These benefits make graphene a viable material for gas detection in this study.

1.2 Problem Statement

The detection, monitoring, and analysis of VOCs is a topic of rising interest in the field of gas sensor development. Even though several gas sensor devices are commercially accessible, there are gaps in the enhanced reliability and sensitivity of sensors for precise environmental monitoring. Most of the available sensors are expensive and suffer from high power consumption, poor stability, inflexibility, and malfunction in harsh environments [7]. Therefore, polymer–based gas sensors have been proven to enhance the performance of gas sensors due to their easy fabrication, low cost, high reproducibility, and flexibility compared to conventional sensors. Chitosan composite can be easily flexed and deformed into various shapes, which are attributed to chitosan molecules that function as dispersion, reduction agents, and support material [17]. In addition, this composite can be attached to paper owing to its adhesive property hence it can be utilized in versatile applications in a disposable manner.

Besides, the rapid expansion of industrialization has resulted in remarkable technological achievements as well as severe negative environmental consequences. Volatile organic compounds (VOCs), which include toxic gases and contaminants produced by industrial processes, are hazardous to the human cardiovascular and respiratory systems. The detection and monitoring of VOC gases such as ethanol and acetone is a critical concern for public health and environmental safety, as prolonged exposure to ethanol vapor at an exposure limit volume of roughly 3.3% - 19% can cause nausea, skin rashes, Parkinson’s disease, and hypotension while exposure to acetone vapor can be harmful to human health and lead to symptoms like bronchitis, weariness, disorientation, and organ damage [18]. Therefore, to improve the sensitivity and efficiency of the gas sensor, chitosan polymer was chosen which also can produce a low-cost polymer gas sensor to detect the presence of VOC gases.

1.3 Objectives of Study

There are two main objectives of this project work enlisted as follows:

i. To develop polymer-based gas sensors for the detection of volatile organic compound gases at room operating temperature.

ii. To analyse the characteristics of polymer-based gas sensors in terms of response, response time, and recovery time.

1.4 Scope of Project

This project only focuses on the following scope and limitations:

i. This project uses graphene as the sensing material, chitosan as the polymer, and Kapton as the substrate.

ii. An interdigitated electrode will deposit onto the Kapton substrate as a first layer using a screen-printing technique.

iii. A silver conductive paste will be used for the interdigitated electrode.

iv. Besides, the sensing film (Gr) will deposit onto the interdigitated electrode using the doctor blade technique as the second layer.

v. The sensing area of this gas sensor will be limited to 1 cm x 1 cm.

vi. This gas sensor only focuses on detecting acetone and ethanol gases.

1.5 Thesis Outline

The fabrication of a polymer-based gas sensor for volatile organic compound gas sensing is done in this project whereby the progress and the result are documented in this thesis. The thesis is structured as follows:

Chapter 1: Introduction

This chapter presents the brief idea of gas sensor implementation and its importance in securing the future of humankind. The problem statement is based on the limitation of the material used to develop the gas sensor. In addition, the objectives and problem statement of this project are discussed as well as to give a brief and essential idea of this project.

Chapter 2: Background Study

This chapter incorporates earlier work done by various researchers on polymer-based gas sensor fabrications to gather knowledge and references on polymer gas sensors. This chapter will also examine several sensing materials used in polymer gas sensors, such as reduced graphene oxide, CNTs, and graphene. In addition, fabrication techniques for this sensor will be discussed in this chapter, such as screen printing, doctor blade, and spin coating. This chapter also will discuss the properties of the polymer gas sensor, such as response, response time, and recovery time.

Chapter 3: Methodology

This chapter describes the procedure for producing a polymer-based gas sensor for VOC gases, including material selection and sensor fabrication. The procedure began with the creation of a polymer solution by dissolving low molecular weight chitosan powder in a 2% w/v acetic acid solution. Following that, the paste was prepared by mixing the polymer solution with the graphene and stirring for 24 hours. The fabrication procedure is then continued by depositing the silver paste as an interdigitated electrode onto the Kapton substrate using screen-printing technology as the first layer of the gas sensor. The sensing material is subsequently printed on the electrode surface using the doctor blade technique, becoming the sensor’s second layer. The gas sensor was put in a gas chamber, and the source meter (Keithley 6487) was used to supply voltage to the sensor. The I-V measurement is required to check the conductivity of the constructed gas sensor before it is exposed to the target gas. The output of the gas sensor was recorded in its current form using the LabVIEW 2010 program.

Chapter 4: Results and Discussion

This chapter presents the results obtained that have been achieved in this project. The I-V characteristic of the gas sensor showed the responsiveness of the sensor toward ethanol and acetone vapor. All the measured characteristics include response, response time, and recovery time. This chapter also discussed the material's physio-chemical characteristics. Scanning Electron Microscope (SEM) and Raman spectroscopy are used to explore the surface morphologies and elemental compositions of graphene at a detailed scale.

Chapter 5: Conclusion

The best results of the polymer-based gas sensor employing graphene composite that meets the characteristic requirement are presented in this chapter. An additional study is being conducted to provide guidelines and recommendations for future improvements in the fabrication of the polymer-based gas sensor for VOC gases.

CHAPTER 2

BACKGROUND STUDY

2.1 General Overview

This chapter demonstrates the journal and research papers on the design workflow of polymer-based gas sensors for detecting VOC gases. A variety of studies and research have been done on polymer-based gas sensor devices, but until today, the best material and method for the sensor do not exist. Each of the journals has its distinct research value. Different materials, methods, and workflows fabricate the gas sensor. The literature review is divided into four Sub-chapter which are previous research that explains the previous research of polymer-based gas sensors, deposition technique of polymer gas sensors (that include screen printing, doctor blade, and spin coating techniques), sensing material (such as reduced Graphene Oxide (rGO), carbon nanotube (CNT), and Graphene) and characteristic of the gas sensor (response,

response time and recovery time). All the sub-chapters are supported by several journals and articles reviewed for a better understanding of polymer-based gas sensors for VOCs gases sensing.

2.2 Polymer-Based Gas Sensor

Table 2.1 lists the properties of the polymer-based gas sensor that was investigated. According to a recent article by Foronda et al. [8], polymer-based sensors have been extensively studied in the field of gas sensing. These polymers, particularly intrinsic polymers, have shown promising surface responses in detecting volatile organic compounds (VOCs) such as ammonia, acetone, formaldehyde, methanol, and ethanol. While numerous commercially available gas sensor devices exist, there are still gaps in reliability, sensitivity, and accurate environmental monitoring. Previous research has demonstrated several advantages of polymers, including ease of synthesis, operation at room temperature, fast response time, and high sensitivity to various gases, making them a highly promising material for gas sensing applications.

To improve the sensitivity and efficiency of gas sensors, diverse materials have been explored in electrical sensors, including nanomaterials, polymers, and carbon materials, as highlighted in research conducted by Park et al. [17]. Carbon materials like graphite, graphene, carbon nanotubes, graphene oxide, and reduced graphene oxide have been frequently employed due to their high conductivity and ability to absorb gas molecules physically. Among various carbon materials, graphene oxide (GO) stands out as a representative carbon material for detecting VOC gases due to its superior sensing affinity compared to others. Meanwhile, chitosan (CS), a natural polysaccharide, readily forms a gel with GO nanosheets. The synthesized GO/CS composite exhibits flexibility and can be easily molded into different shapes. Chitosan molecules act as dispersion and reduction agents and provide support, allowing the composite to adhere to paper surfaces, making it suitable for versatile applications with a disposable nature.

As for the deposition technique, the drop-casting technique is widely used in the fabrication of polymer-gas sensors. It is an effective and simple process used to deposit sensing materials onto the substrates for application in gas sensors. The drop-casting method was an alternative to working with polymer semiconductors, which were costly and did not dissolve easily.

Table 2.1: Characteristics of polymer-based gas sensor

Sensing material	**Polymer**	**Substrate**	**Gas**	**Method**	**Response time (s)**	**Citation**
Zinc Oxide (ZnO)	Polyaniline (PANI)	Telfon	Ammonia, Acetone, Methanol, Ethanol	Drop-casting	Methanol 8-10s	[8]
Reduced Graphene Oxide (rGO)	Poly (3-hexylthiophene) (P3HT)	SiO$_2$/Si	Methanol, Acetone, Ethanol	Spin Coating	Ethanol 50s Acetone 44s	[19]
Graphene Oxide (GO)	Parylene C (poly(pxylylene))	Glass	Methanol, Ethanol, Propanol, Pentanol, Hexanal, Toluene	3D Printing, Spin Coating	Ethanol 146s	[20]
Graphene Oxide (GO)	Polyvinylidene difluoride (PVDF)	CNT Aerogel	Ethanol, argon, hydrogen	Chemical/ Spray Coating	Ethanol 150s	[21]
Reduced Graphene Oxide (rGO)	Chitosan (CS)	Overhead projector film, commercial A4 coated paper, cellulose paper	Nitrogen dioxide (NO$_2$)	3D printing, drop-casting	Nitrogen 76.37%	[17]
Zinc Oxide (ZnO)	Chitosan (Cs), polyvinylpyrrolidone (PVP)	Polymeric, SiO$_2$	Hydrogen	Drop-casting	Hydrogen 24%	[22]

Glycerol Ionic liquid (IL)	Chitosan (CS)	Copper sheet	Hydrogen Sulfide (H_2S)	Drop-casting	Hydrogen Sulfide 15s	[7]
Tin Oxide SnO_2, reduced Graphene Oxide (rGO)	Polyaniline (PANI)	Flexible polyethylene terephthalate (PET)	Hydrogen Sulfide (H_2S)	Drop-casting, screen printing, In situ polymerization	Hydrogen Sulfide 9.1%	[23]
Vanadium pentoxide (V_2O_5)	Polyanisidine (POMA)	Glass	Ammonia	Layer-by-layer (LbL), deposition method	Ammonia 15s	[24]
Graphene Oxide (GO)	Poly (methyl methacrylate) (PMMA)	Glass	Methane	Hummers, Spin-coating	Methane 10s	[25]

2.3 Deposition Technique of Polymer-Based Gas Sensor

The structural and morphological features of the sensing layer's surface substantially influence the performance of polymer-based gas sensors. This layer controls the absorption and desorption of oxygen and gas molecules, as well as the carrier mobility. As a result, deposition techniques play an essential role in growing films with superior gas sensing capabilities. As a result, much research on gas sensors has been concentrated on this area [26].

2.3.1 Drop Casting Deposition

Drop casting was employed to create small coatings on tiny surfaces. It required only a small amount of solvent. When multiple droplets were formed using this method, they provided a distinctive environment to control the shrinkage direction and the evaporation rate of the droplets [27]. In this method, a solution was poured onto the substrate as drops and was allowed to dry without spreading [28]. When the droplets were projected onto the substrate, the liquid first spread on the surface from the drop locations due to the interfacial forces that inclined to drive the droplet outward. As multiple droplets were cast onto the substrate surface, when the edges of the droplets came in contact with each other, they mixed, forming a noncircular drop with a concave contact line. The schematic of the drop-casting method is shown in Figure 2.1.

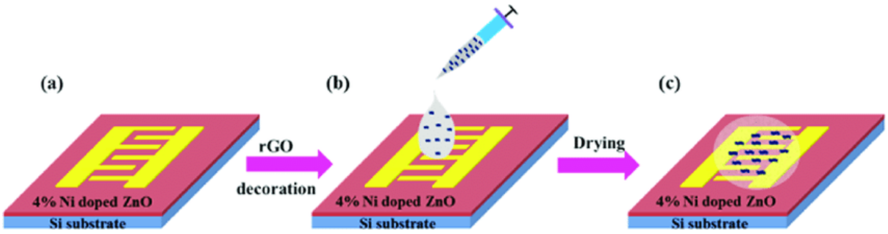

Figure 2.1: Drop casting deposition technique [29]

Previous findings discovered that drops with shapes other than circles dried unevenly [30]. They found that these drops had areas that stuck out a lot, dried up faster, and ended up with more material deposited. The process called capillary flow, which is like how liquid moves between the droplets, was responsible for this uneven deposition at the contact line. This meant that they could figure out and control how the material was deposited, even if they did not know the exact chemicals involved in the solution, liquid, or surface. However, using this method could lead to films that were not consistent because the drying conditions were not the same everywhere, making it difficult to control. These films ended up being thicker in the middle and thinner at the edges. The drop casting method was a different way to work with polymer semiconductors, which were costly and did not dissolve easily.

2.3.2 Screen-Printing Deposition

Screen printing is classified as a printing technique. In printing procedures, the paste was placed on a pattern screen and squeezed to transfer the paste to the substrate surface in reverse. In most applications, the screen-printing technology consists of a screen made of synthetic fibre or metal wire and attached to a sturdy steel or aluminium frame with a rectangular plane [31]. After putting the correct amount of paste into the frame, it is scraped across the surface of the screen using a squeegee at a steady rate. Squeegee pressure is used to transfer paste material into the substrate by following a pattern drawn on a screen. As a result, the design is transferred to the substrate and a layer of paste is deposited. This printing procedure yields film with a width of 2 - 4 µm. It also regulates the film's transparency and porosity by altering (i) the thread parameters in the screen, such as diameter, counts, and distance between two threads, and (ii) the pressure and speed applied to the squeegee [32]. This technique reduces coating material loss and produces a highly viscous dense film. This feature is ideal for large-scale manufacturing and provides good film quality or uniformity. Because of its better thickness homogeneity, smooth operation, and speedier industrial application, screens are widely used. This approach has some disadvantages, including a greater wet thickness, high viscosity needs, and poor volatility [31]. Previous research [33] has proved the effectiveness of using screen printing techniques toward the functionalized MWCNT-PEDOT: PSS-based solution. The fabricated polymer-based gas sensor showed good performance of the recovery property. Figure 2.2 illustrates the screen-printing technique.

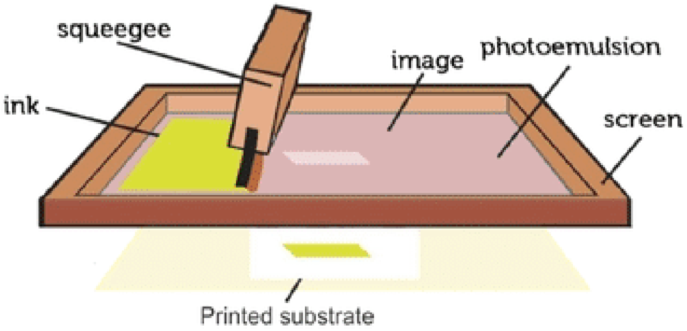

Figure 2.2: Screen-printing deposition technique [34]

2.3.3 Doctor Blade Deposition

Doctor blades are classified as coating techniques. The paste flows through the blade on the substrate surface in coating processes as in Figure 2.3. The doctor blade approach is based on Glen Howatt's process for manufacturing ceramic capacitors [31]. This technique can also be used to create films in PSCs, OSCs, and DSSCs [35]. The blade is displaced over the substrate at a consistent velocity with a specific contact angle and height in this process. The movement of the blade uniformly distributes the paste onto the substrate, resulting in a fixed thick film. The layer thickness obtained with this procedure is in the range of 10 - 500 µm. This approach is less expensive and reduces particle loss by about 5 % when compared to spin-coating. As a result, a small number of fundamental materials is sufficient for this procedure. This technology is suitable for mass production and has become one of the most straightforward and cost-effective approaches for the deposition of semiconductor oxide paste and modem electronics. This approach has various advantages, but the main disadvantage is its slow evaporation or ability to accumulate at high paste concentrations.

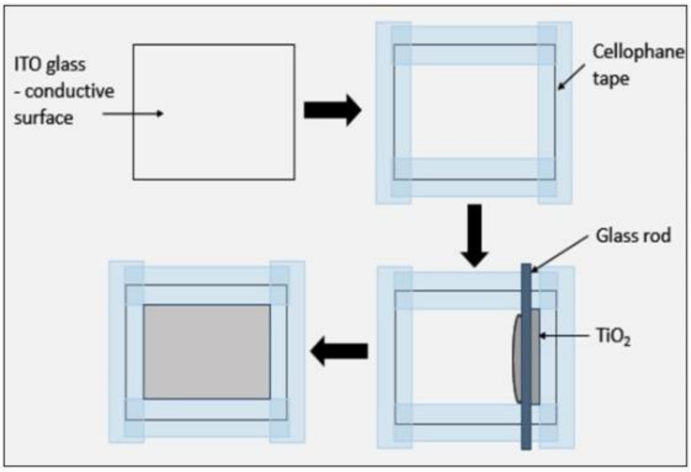

Figure 2.3: Doctor Blade deposition technique [36]

2.3.4 Spin Coating Deposition

Spin coating is a technique used in thin film fabrication to deposit a uniform layer of organic compounds on flat surfaces. Spin coating is usually done in four steps: deposition, spin-up, spin-off, and evaporation [37]. The material is placed on the turntable in the first stage, followed by spin-up and spin-off in sequence, while the evaporation stage proceeds throughout the process. Centrifugal force distributes the applied solution on the turntable. The layer thins as the spinning speed increases. The applied layer is dried after this stage. Because of the quick rotation, uniform evaporation of the solvent is achievable [38]. Evaporation or simply drying removes the high volatile components of the solution from the substrate, while the low volatile components of the solution stay on the surface of the substrate. The thickness of the deposited layer is determined by the viscosity of the coating solution and the rotational speed. Spin coating is a widely used technique for creating thin polymer film coatings that are highly homogeneous and highly reproducible over both tiny and large surfaces. The spin coating technique has been thoroughly explored and used in many possible fields including gas sensors due to its many benefits, including low cost, excellent homogeneity, superior control, and molecular and atomic order of the constituent particles [38]. Research [19] proved that the fabrication of P3HT/rGO composite films using the spin coating technique exhibited outstanding sensitivity to acetone and ethanol vapor. The size of the substrate is one of the key disadvantages of spin coating. Because film thinning becomes more difficult as the size grows, high-speed spinning becomes more challenging. The spin coating has a very low material efficiency. In general, 95% - 98% of the material is hurled off and discarded throughout the process, with only 2% - 5% being discharged onto the substrate [39]. Figure 2.4 shows the fabrication of an ammonia gas sensor using the spin coating technique.

Figure 2.4: Ammonia gas sensor using spin coating technique [40]

2.4 Sensing Material

The selectivity of the sensing material is a crucial consideration in the manufacturing of a gas sensor. A good sensing material should have high sensitivity, fast response and recovery, and good selectivity [41]. The development of low-cost, dependable sensing devices for gas detection, particularly at room temperature, continues to be a key scientific and technological challenge [42]. Gas sensors based on various sensing materials and methodologies are categorised based on the detection method. As 2D materials, graphene, transition metal chalcogenides, boron nitride, transition metal carbides/nitrides, metal-organic frameworks, and metal oxide nanosheets indicate future gas-sensing materials [38], [39].

2.4.1 Reduced Graphene Oxide (rGO)

Due to their distinctive structural characteristics, exceptional thermal and electrical properties, and mechanical strength, carbon materials like graphite, graphene, carbon nanotubes, graphene oxide, and reduced graphene oxide (rGO) have been widely used in a variety of applications, including energy, catalysis, environmental monitoring, and sensors [43]. rGO has drawn significant attention as an active material in gas sensors because of its electrical properties and large surface area for adsorption and interaction with gas molecules [44]. These advantages allow rGO-based gas sensors to exhibit good sensitivity and rapid response/recovery behaviour when compared to well-established analytical techniques like gas chromatography and spectroscopic approaches [45]. In general, rGO is produced by reducing the oxygen-containing functions of GO generated via the Hummers' graphite oxidation process [45] GO is composed of sp2 hybrid carbon networks that have reactive oxygen functionalities such as epoxy, hydroxyl, and carboxyl [46]. Reduction can be achieved through chemical or thermal treatment. rGO, on the other hand, has limitations for large-scale practical use in sensing devices due to its low processability [47]. Combining rGO with polymer composites has recently been presented as a viable strategy to solve this issue [47]. rGO can be altered to carry essential functional groups compatible with polymers by utilising some of its residual oxygen capabilities. Further charge exchange interactions between rGO and polymers are thus possible. Furthermore, due to its polar functional groups, rGO can form significant interactions with gas analytes via dipole-dipole interactions, van der Waals forces, and hydrogen bonding. As a result, rGO can be injected into a polymer matrix and used to build gas in this situation, rGO acts as a receptor material to mediate strong interactions between the polymer matrix and analytes [46]. Previous research [48] used a PEDOT/rGO nanocomposite to effectively build a highly sensitive and selective carbon monoxide gas sensor. This research establishes graphene oxide as a viable material capable of improving the performance of polymer-based gas sensors [45].

2.4.2 Carbon Nanotube (CNT)

Carbon nanotubes (CNTs) have been studied as gas-sensing materials for over 20 years [49], [50]. They are multi-walled (MWCNTs) or single-walled (SWCNTs) seamless cylinders formed by wrapping graphene sheets along the axial direction [51]. Carbon nanotubes offer a high surface-to-volume ratio, superior chemical and mechanical stability, and electrical qualities appropriate for gas sensing applications [52]. As a result, they are positioned as next-generation gas sensors capable of making a difference in the gas sensing market [53]. CNTs are sensitive towards strong electrons CNTs are susceptible to strong electron withdrawing or donating gases like NH_3 and NO_2. There are technological impediments to their commercialization. Their synthesis is expensive and laborious since it is difficult to generate continuously defect-free nanotubes [54]. Another concern is the interaction of the CNT surface with oxygen/water molecules, which can affect the sensor's responsiveness to target gases. UV light illumination is one approach for dealing with this issue [53]. When CNTs are exposed to gas molecules, their electrical characteristics change due to charge transfer between the nanotubes and molecules (functioning as electron donors or acceptors). Because the preparation process and technique have a considerable impact on sensor behaviour and properties, modifications can be critical for the stability of carbon nanotube-based systems. Another downside of CNT gas sensors is their delayed response and recovery due to the nature of the gas adsorption and desorption processes [54]. In addition to research on gas sensors employing SWCNTs and MWCNTs, such as MWCNTs for hydrogen detection [55], research on embedding CNTs into diverse matrix materials has been conducted. Polymers such as multi-walled carbon nanotubes (MWCNTs) supplemented with PEDOT and PANI obtained strong ammonia selectivity but poor recovery [56], and metal oxides such as MWCNT/SnO_2 composites for detecting hydrogen or NO_2 at ambient temperature. The decoration of CNTs with noble metal nanoparticles has resulted in increased gas sensing response to some gas molecules, such as SWCNTs coated with Pd's improved sensitivity to H_2 [57].

2.4.3 Graphene

Applications for graphene, a one-atom-thick sheet of carbon atoms with a hexagonal crystal structure in two dimensions, appear promising for gas sensors [58]. Because of its unique properties, such as a high surface-to-volume ratio, graphene, and its derivatives have attracted a significant deal of attention due to their higher adsorption capacity for gas molecules and strong surface activity [59]. Graphene is a two-dimensional material with various desirable features, including low room temperature resistance, rapid electron mobility (200,000 $cm^2V^{-1}\ s^{-1}$), a large surface area, and a high carrier density ($10^{12}\ cm^{-2}$). When a small amount of gas is deposited on the surfaces of graphene sheets, it can minimise electrical noise and produce a change in resistance. The fundamental feature is that all atoms in a graphene sheet can be considered surface atoms, meaning that they are all capable of adsorbing gas molecules, resulting in a very wide surface area available for the sensing mechanism.

Furthermore, the interaction between graphene layers and adsorbate molecules can vary in intensity, depending on whether it is van der Waals or covalent bonding. It is also distinguished by an exceedingly slight change in resistance as a result of very low concentrations of gas adsorption, allowing gas detection down to the molecule level.

Despite recent advances in graphene-based gas sensors, sensing performance remains inadequate in practice. Graphene-based sensors, in general, are always sensitive to more gases. Another problem with most graphene-based sensors is their lack of reversibility. Another drawback is their inability to be used in large-scale practical applications in gas sensors due to their low processability.

2.5 Characteristics of Polymer-Based Gas Sensor

The characteristics usually used to identify the sensor performance include response, response time, and recovery time.

2.5.1 Response

The gas response is defined as the ratio of the resistance of the sensor in a flow of synthetic air, $\boldsymbol{R_a}$, and the steady-state resistance of the sensor in the analyte gas flow, $\boldsymbol{R_g}$ $[\mathbf{57}]$. The response of the sensor can be obtained using Equation 2.1:

$$\boldsymbol{Response}\ (\%) = \frac{|\boldsymbol{R_a} - \boldsymbol{R_g}|}{\boldsymbol{R_a}} \times \mathbf{100} \qquad \text{Equation 2.1}$$

Where:

(R_{gas}): Electrical resistance

$(R_{air)}$: Resistance in dry air

2.5.2 Response and Recovery Time

The other two essential characteristics of a gas sensor are response time and recovery time. When a reducing or oxidising gas is introduced, the response time (τ_{res}) of a gas sensor is defined as the amount of time it takes for the sensor to achieve 90% of its maximum or minimum conductance value [61]. When the flow of reducing or oxidising gas is stopped, the recovery time (τ_{rec}) is defined as the amount of time needed to return to within 10% of the initial baseline [62]. A gas sensor's response time is determined by several factors, including the sensor's design, technology, and the nature of the gas being detected. Response times might vary greatly between sensor kinds and brands. The time it takes for the sensor's output to reach a particular percentage of its final value in response to a step change in gas concentration is commonly characterised as the response time. The recovery time is a measure of how quickly the sensor recovers its sensitivity and stability after being exposed to the gas. The response and recovery time can be varied on certain conditions such as temperature, humidity, and the presence of other gases. Furthermore, the response properties of different sensor technologies, such as electrochemical, semiconductor, or optical sensors, may differ. When comparing gas sensors or determining their suitability for certain applications, it is critical to consider both sensitivity and response time, as both factors affect the sensor's capacity to detect and respond to changes in gas concentration in a fast and correct manner.

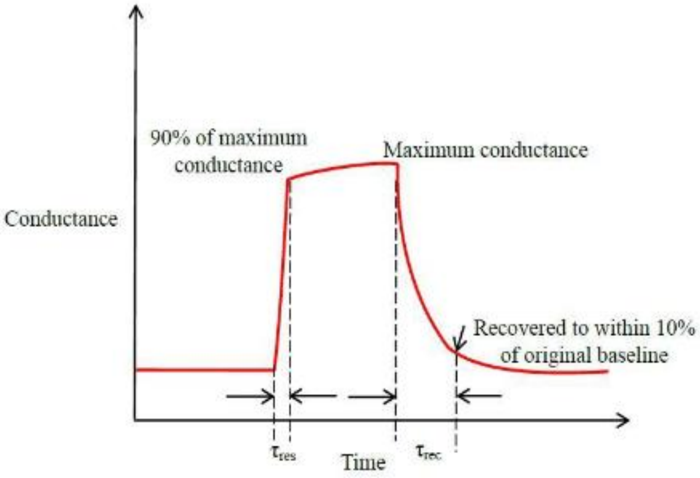

Figure 2.5: Calculation of response time and recovery time [61]

2.5.3 Mechanism of Graphene Gas Sensor to Ethanol and Acetone

To discern the superior response of graphene adorned with Ag_2S nanoparticles to acetone gas, the underlying mechanism was investigated by initially calculating the binding energies between gas molecules and an Ag_2S slab. Figure 2.6 illustrates the binding energies of gas molecules in acetone/ Ag_2S, ethanol/ Ag_2S, and hexane/ Ag_2S model systems. The binding energy (BE) was determined as $E_{Binding} = E_{gas-molecule/slab} - (E_{gas-molecule} + E_{slab})$ where $E_{gas-molecule/slab}$ represents the total energy of the Ag_2S slab with the adsorbed gas molecule, and $E_{gas-molecule}$ and E_{slab} denote the total energies of the individual gas molecule and Ag_2S slab, respectively. Generally, a larger contact area between the molecule and slab surface results in a greater binding energy. Surprisingly, despite acetone and ethanol having smaller contact areas than hexane, they exhibited higher binding energies. To delve into this inconsistency, charge density differences for the three model systems were calculated using $\rho = \rho_{gas-molecule/slab} - (\rho_{gas-molecule} + \rho_{slab})$ are the electron charge densities of the Ag_2S slab with the adsorbed gas molecule, the gas molecule alone, and the Ag_2S slab alone, respectively.

The charge density difference analysis revealed the most significant electron transfer in the acetone/ Ag_2S system. In Figure 2.6 (b), red and green surfaces (±3.375 × 10−3 e/A) signify electron charge accumulation and depletion zones, respectively. Notably, electrons accumulated over extensive regions of the Ag_2S surface with adsorbed acetone molecules. Additionally, electron transfer and redistribution within the acetone molecule were observed. Conversely, for ethanol and hexane molecules (Figure 2.6 (c) and (d)), smaller regions of electron transfer and redistribution were evident.

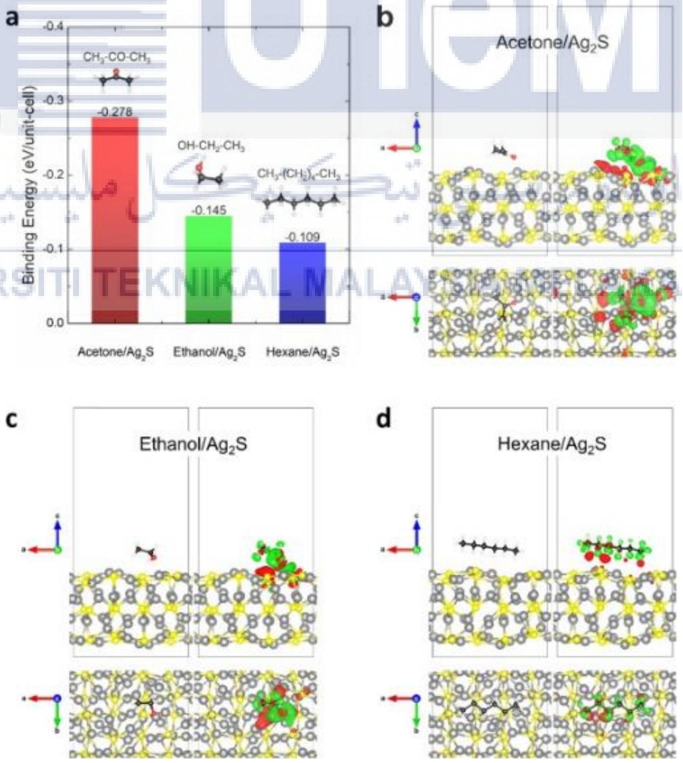

Figure 2.6: Optimized structures (left) and charge density difference plots (right) for (b) acetone/Ag_2S, (c) ethanol/Ag_2S, and (d) hexane/Ag_2S

CHAPTER 3

METHODOLOGY

3.1 General Overview

This chapter describes the procedure for fabricating a polymer-based gas sensor for VOC gases, including material selection and sensor fabrication. The procedure began with the creation of a polymer solution by dissolving low molecular weight chitosan powder in an acetic acid solution. Following that, the paste was prepared by mixing the polymer solution with the graphene. The fabrication procedure is then continued by depositing the silver conductive interdigitated electrode onto the Kapton substrate using the screen-printing technique as the first layer of the sensor. The sensing material is subsequently coated on the electrode surface using the doctor blade technique, becoming the second layer of the sensor. The I-V measurement is required to check the conductivity of the constructed gas sensor before it is exposed to the ethanol and acetone gases.

3.2 Flowchart

The methodology and development process of polymer-based gas sensors for VOC gases can be summarized and illustrated in the following flow chart in Figure 3.1. First and foremost, this project starts with preparing the polymer solution by mixing the chitosan with the acetic acid (2% w/v solution) while stirring to create a uniform viscous solution. Then, the solution will be combined with the graphene using various ratios to get a suitable paste that can respond to the ethanol and acetone vapours. As for the fabrication of the gas part, an interdigitated electrode will be deposited onto the Kapton substrate as a first layer using a screen-printing technique. A silver conductive paste will be used for the interdigitated electrode. Besides, the sensing film (Gr) will be deposited onto the interdigitated electrode as the second layer using the doctor blade technique. The step will continue with the I-V characteristic. The gas sensor will then be tested with the I-V characteristic for its responsiveness to ethanol and acetone gases. The sensor's response, response time, and recovery time are all measured to verify its effectiveness. If the sensor does not respond to the vapor, the operating process will start again by preparing a new paste with any conductivity. The last process is the characterization of SEM & Raman. Physio-chemical characterization will be performed using a scanning electron microscope (SEM), and Raman to investigate surface morphologies and chemical positions of graphene on a detailed scale.

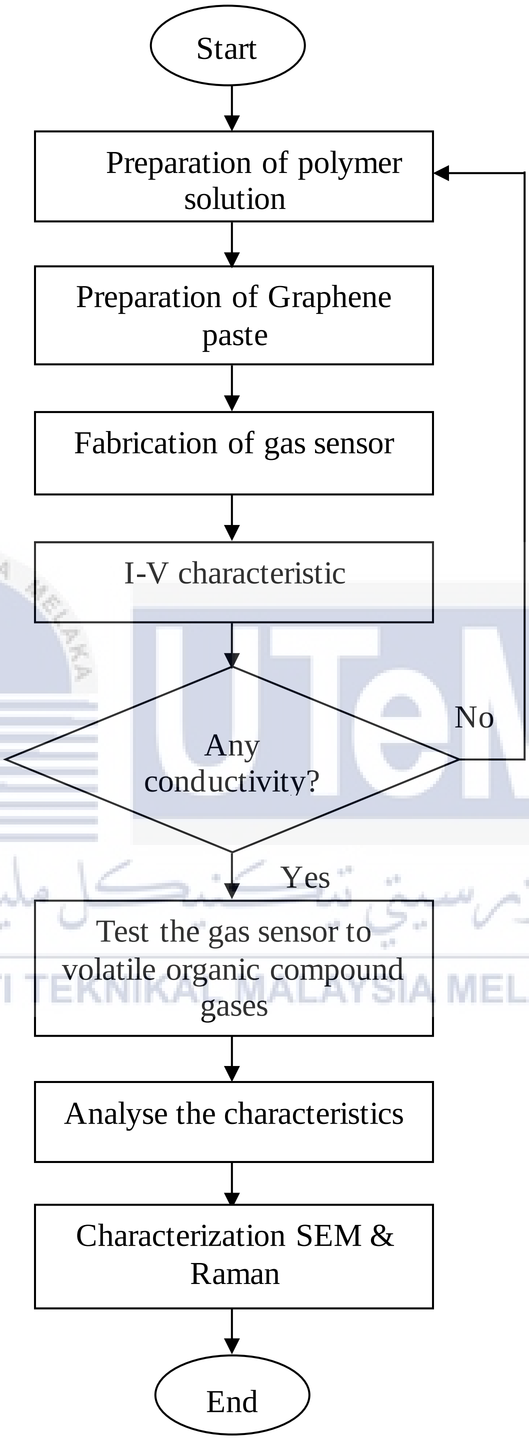

Figure 3.1: The flowchart of the project

3.3 Preparation of Polymer Solution as a Binder

Two different binders were used in this project. The first binder is adapted from previous research [63], and the second binder is the proposed binder to investigate the performance of polymer toward ethanol and acetone gases. Chemiz supplied several materials used with the specification of chitosan (100 g weight, De-Acetylation min 90%) and acetic acid (1L, 2% w/v solution). Initially, 0.2 g and 0.5 g were dissolved into 20 ml acetic acid solution to make polymer solution A as shown in Figure 3.2, and polymer solution B as shown in Figure 3.3, respectively. Next, the solutions were heated and stirred at 100 °C and 500 rpm in 3 hours to make 10 ml of polymer solution. The solutions were cooled to room temperature before further sample preparation.

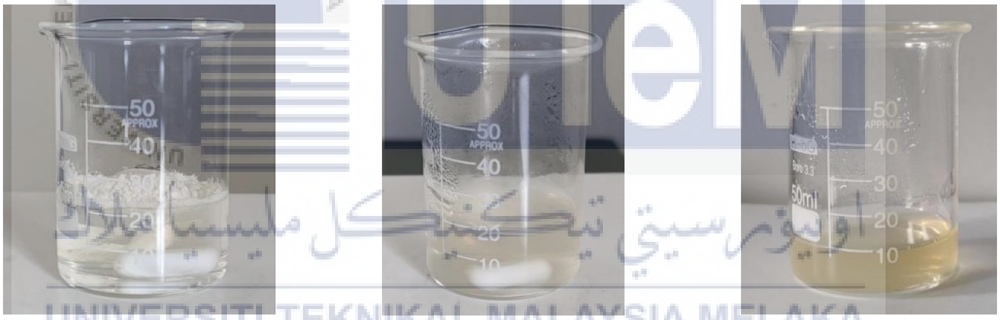

(a) (b) (c)

Figure 3.2: (a) 0.2 g chitosan + 20 ml acetic acid, (b) dissolved polymer, (c)10 ml of binder after stirred at temperature 100 °C and 500 rpm

(a) (b) (c)

Figure 3.3: (a) 0.5 g chitosan + 20 ml acetic acid, (b) dissolved polymer, (c) 10 ml of binder after stirred at temperature 100 °C and 500 rpm

3.4 Preparation of Graphene Paste as a Sensing Layer

Firstly, 4.75 ml of solutions are mixed with 0.25 g of graphene for each solution to make paste A and paste B. The mixtures were stirred at 40 °C and 80 rpm for 24 hours. Figure 3.4 illustrates the process of preparing the graphene paste A, while Figure 3.5 illustrates the process of preparing paste B.

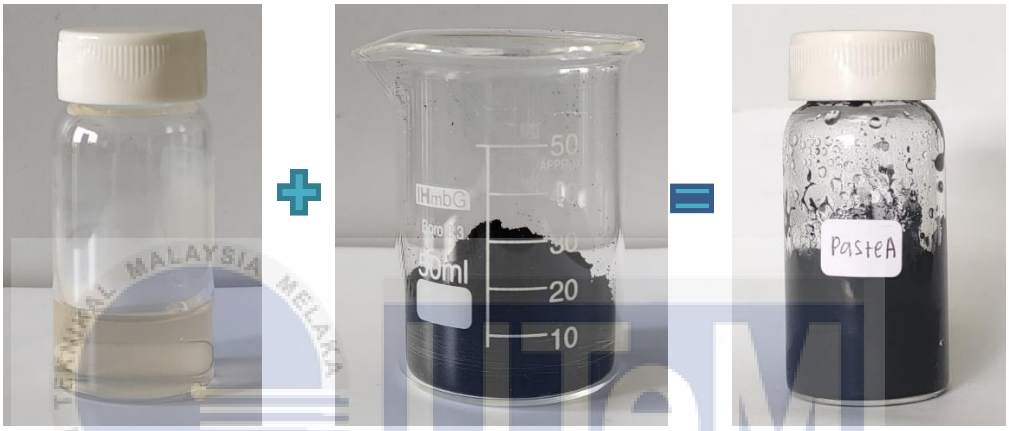

(a) (b) (c)

Figure 3.4: (a) 4.75 ml of polymer solution A, (b) 0.25 g of graphene, (c) Paste A after mixtures of polymer solution A and graphene

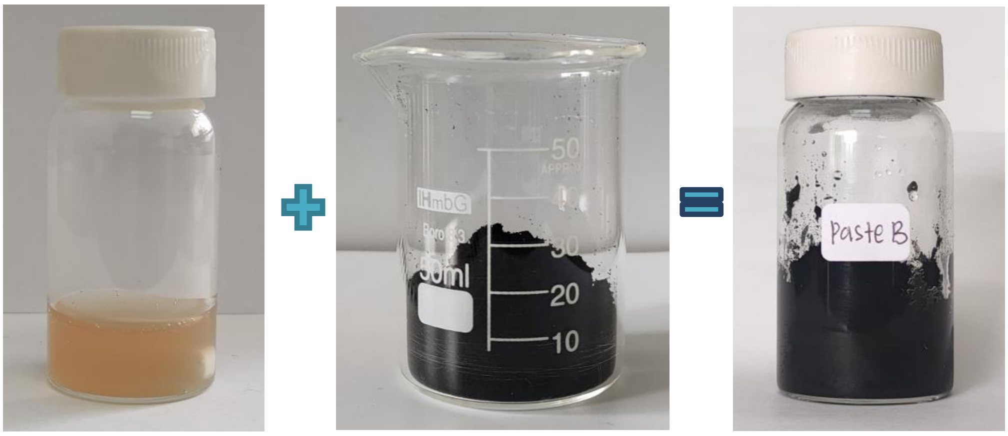

(a) (b) (c)

Figure 3.5: (a) 4.75 ml of polymer solution B, (b) 0.25 g of graphene, (c) Paste B after mixtures of polymer solution B and graphene

3.5 Fabrication of Polymer-Based Gas Sensor

There are two different techniques to fabricate the polymer gas sensor. Screen printing technique was performed to print the electrode on the Kapton substrate in the first layer, while the doctor blade technique was applied to deposit the sensing material for the second layer of the polymer-based gas sensor.

3.5.1 Electrode Deposition of Polymer-Based Gas Sensor

Kapton film substrates were used as the substrate of the gas sensor. The substrate was cut into 2 cm x 2 cm. The interdigitated electrode (silver) was deposited onto the Kapton substrate using a screen-printing technique. Firstly, an amount of silver paste was placed into the frame, then the paste was scraped across the screen's surface using a squeegee. Squeegee pressure transfers paste material into the substrate by following a pattern on the stencil. As a result, the design is transferred to the substrate, and a paste layer is deposited. The electrode was then annealed at 150 °C for 10 minutes in the oven.

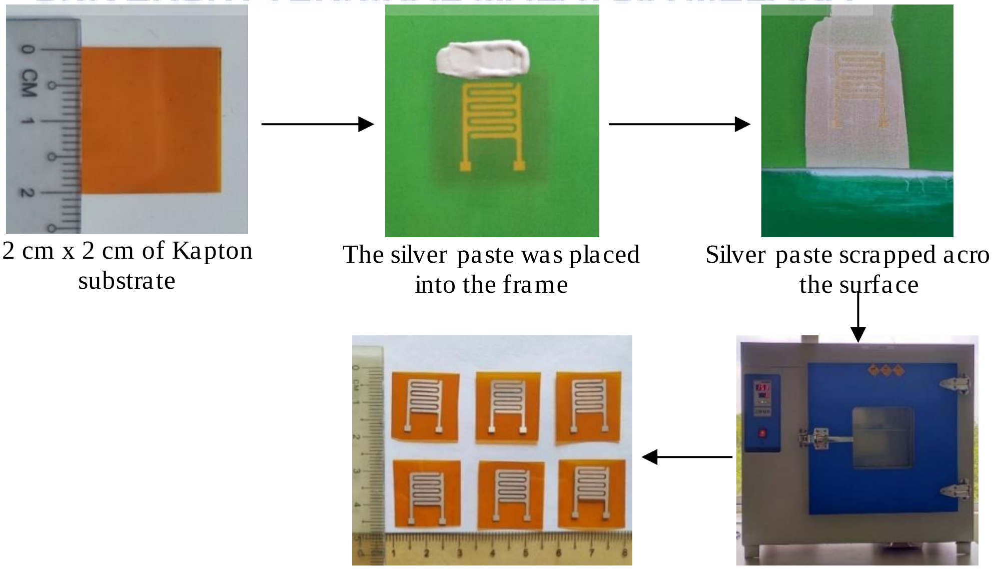
2 cm x 2 cm of Kapton substrate

The silver paste was placed into the frame

Silver paste scrapped across the surface

Annealing at 150 °C for 10 minutes

The printed electrode

Figure 3.6: The electrode fabrication process using a screen printing technique

3.5.2 Sensing Layer Deposition Of Polymer-Based Gas Sensor

The sensing material paste that has been prepared in section 3.4 was coated onto the printed electrode using the doctor blade technique. This technique is done by placing an amount of graphene paste then deposited on the sensor surface and spread to provide a homogeneous sensitive layer at 1 cm². The area on which the material was deposited was controlled by developing a 1 cm^2 of area using scotch tape. The squeegee was placed over the substrate at a consistent velocity with a specific contact angle and height in this process. The movement of the squeezer uniformly distributes the paste onto the substrate, resulting a thick film gas sensor. Lastly, the sample was annealed at 150 °C for 30 minutes in the oven. Figure 3.7 illustrates the fabrication of a polymer-based gas sensor using the doctor blade technique. This procedure was applied for both paste A and paste B, with two variables coated by one layer of sensing material and another by two layers of sensing material to cover the entire sensing area.

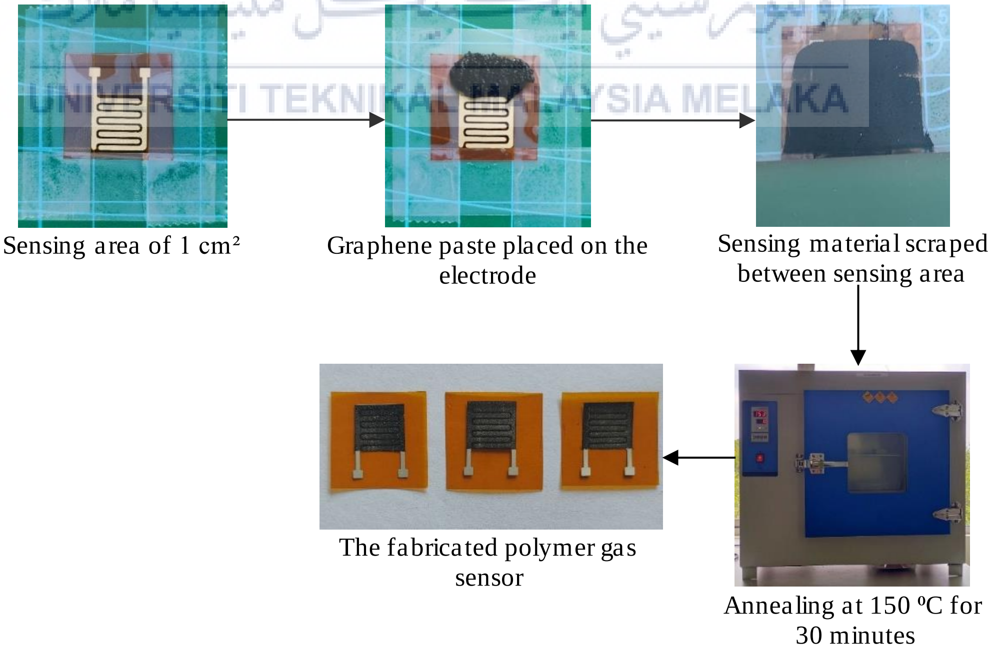

Figure 3.7: The fabrication of polymer gas sensor using the doctor blade technique.

3.6 I-V Characteristic Measurement

Figure 3.8 shows the setup of the current-voltage (IV) measurement for the polymer-based gas sensor. The polymer gas sensor was placed in a gas chamber, and supply voltage was supplied to the gas sensor using the source meter (Keithley 6487). The I-V measurement needs to be carried out to check the conductivity of the fabricated gas sensor before exposure to the target gas. The output of the gas sensor was captured in a current form and was recorded using the LabVIEW 2010 software.

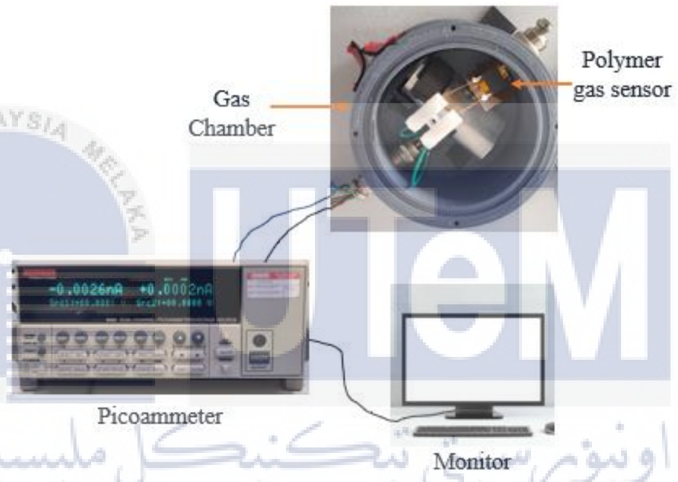

Figure 3.8: I-V measurement for polymer-based gas sensor

3.7 Experimental Setup of Acetone and Ethanol Measurement

Figure 3.9 depicts the experimental setup for measuring gas sensor response to acetone and ethanol. The acetone solution was fill in glassware, and the vapor is flowed inside the gas chamber via a silicone hose. The acetone solution was made by mixing 25 ml of acetone with 25 ml of distilled water with a magnetic stirrer at 100 rpm for 5 minutes. The solution is then heated to 120 °C for 30 minutes to produce acetone vapor.

To generate ethanol vapor, the identical process is done using ethanol and distilled water.

The gas sensor's current was initially monitored for 15 minutes to ensure that it had stabilised at standard atmospheric pressure. After that, the gas chamber's hose was connected to the acetone vapor for 30 minutes, and the response time was recorded. The glassware's hose was withdrawn from the gas chamber after 30 minutes, and the recovery time was recorded. Using the Origin 2019b program, all of the data obtained from the LabVIEW 2010 program were plotted and analysed.

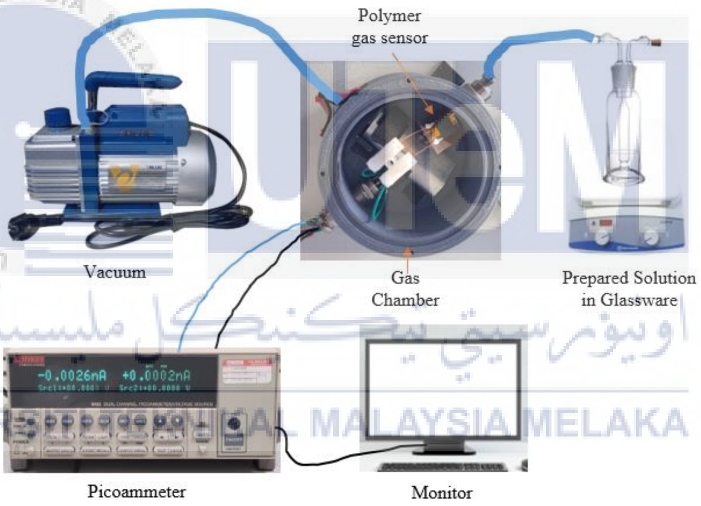

Figure 3.9: Gas measurement setup for polymer-based gas sensor to acetone and ethanol vapor

CHAPTER 4

RESULTS AND DISCUSSION

4.1 General Overview

This chapter presents the results obtained that have been achieved in this project. The I-V characteristic of the gas sensor produced a linear shape, indicating that it can be exposed to gas. Next, current measurement was done by applying 1 V of voltage to measure the sensor's response toward acetone and ethanol. All the measured characteristics, including response, response time, and recovery time, verified its effectiveness. This chapter also describes the properties of a scanning electron microscope (SEM) used to investigate the surface morphology of graphene, which is verified as nanoflake shape, and Raman, which is used to confirm that the sensing material is still graphene after throughout the fabrication process.

4.2 Fabrication of The Polymer-Based Gas Sensor

Figure 4.1 shows the fabricated polymer-based gas sensor based on paste A that containing 5% of the polymer. The thickness of T1-1 (a) was approximately 10 µm according to the scotch tape thickness, while T1-2 (b) was approximately 20 µm due to the double layer deposition. The mixture of T1-paste is quite runny, making it hard to attach when printed onto the electrode which can be seen in T1-1-S3. In addition, the T1-2 paste was thicker than T1-1 paste, which caused the surface of the sensing layer of the gas sensor was cracked after annealing process. Regardless of the number of layers, the two layers deposited showed more consistent and deeper blackness, suggesting better coverage. The details about the sample name can be referred to in the Appendix A of this report.

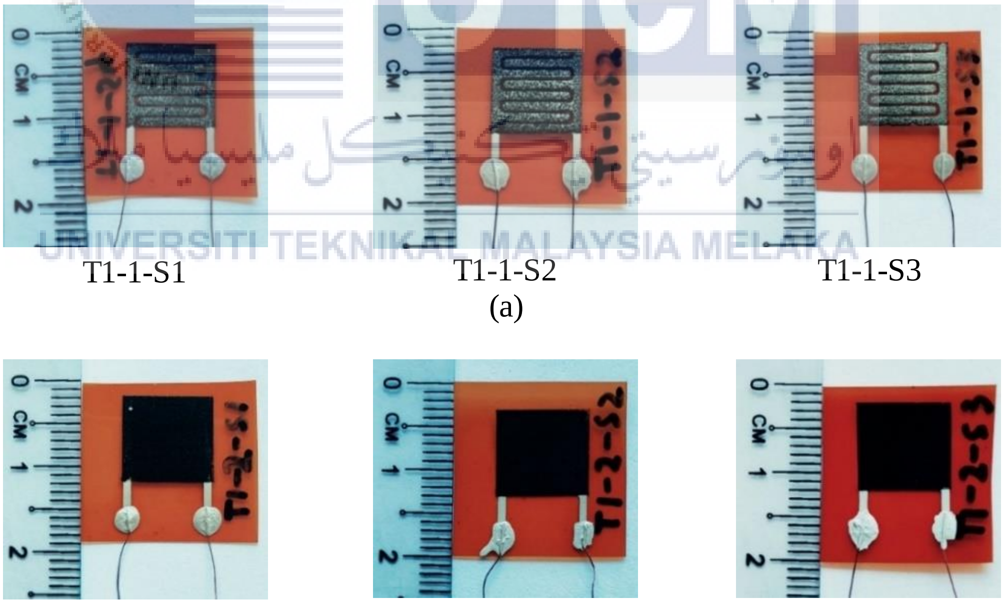

T1-1-S1 T1-1-S2 T1-1-S3
(a)

T1-2-S1 T1-2-S2 T1-2-S3
(b)

Figure 4.1: Fabricated polymer-based gas sensor, (a) Paste A-1 layer, (b) Paste A-2 layer

The fabrication of the polymer-based gas sensor based on paste B with 5% polymer is depicted in Figure 4.2. The thickness of the sensing material indicates that

T2-1 was approximately 10 µm thick, whereas T2-2 was approximately 20 µm thick because of the double layer deposition. This is because of paste B combination was thicker than paste A, make it is easier to place onto the Kapton film. Nevertheless, the T2-2 sample was thicker than the T2-1 sample, and after annealing process the sample's surface was fractured. Regardless of the number of layers applied, two of them T2-1 and T2-2 had deeper and more consistent blackness, indicating better coverage.

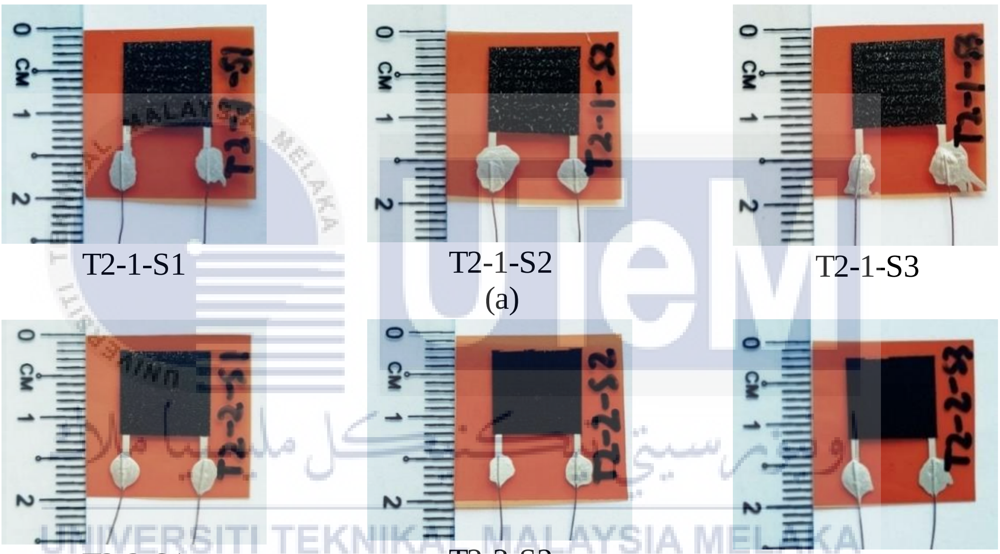

T2-1-S1 T2-1-S2 T2-1-S3

(a)

T2-2-S1 T2-2-S2 T2-2-S3

(b)

Figure 4.2: Fabricated polymer-based gas sensor, (a) Paste B-1 layer, (b) Paste B-2 layer

4.3 I-V Characteristic Measurement

Figure 4.3 depicts the I-V characteristics at 1 V for all the gas sensors built on Kapton film. It consists of four sample sets, which are T1-1, T1-2, T2-1, and T2-2. Every set consists of three samples need to produce a linear graph which is compulsory procedure required for gas exposure. The linear I-V characteristic shows that this sensor behaves electrically according to the Ohm's law, which states that current (I) is inversely proportional to voltage (V). The breakdown voltage for all samples occurs at 5 V as shown in Appendix B,C,D,E. The I-V characteristic of the fabricated gas sensor must be linear to validate that the gas sensor followed the Ohm's law and was likewise a resistance-based gas sensor. Only a conductive gas sensor can be exposed to the target gas for a resistance-based gas sensor. The results indicated that all the gas sensors were conductive based on a linearity graph, implying that all samples may be subjected to ethanol and acetone vapor. The resistance values for T1-1, T1-2, T2-1, and T2-2 were almost identical, meaning the amount of graphene paste deposited using the Doctor blade was nearly similar.

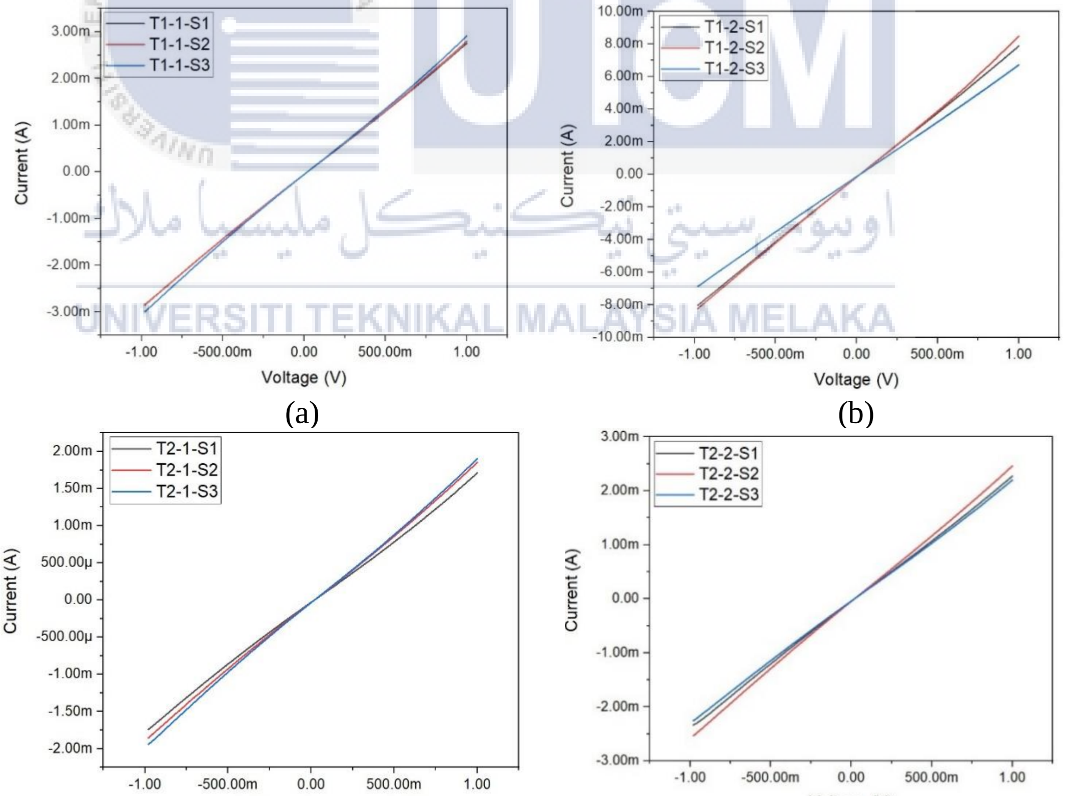

(a) (b)

(c) (d)

Figure 4.3: I-V characteristic of the polymer-based gas sensor at -1V to 1V, (a) T1-1, (b) T1-2, (c) T2-1, (d) T2-2

Table 4.1 displays all the resistance of the fabricated gas sensors. The resistance value of paste B is higher than paste A due to the 2% chitosan used to fabricate the polymer solution B compared to 1% chitosan in polymer solution A. The resistance value of the single layer for both pastes A and B showed a higher value than the double layer. This is because of double layer gas sensor was annealed in twice and it can affecting the amount of polymer that being evaporated. As can be seen, T1-2-S2 generated the lowest resistance, 120.92 Ω, whereas T2-1-S1 generated the highest resistance, 591.72 Ω. The amount of chitosan and layer deposited on the gas sensor's detecting layer contributed to the resistance value. The high chitosan amount influenced the high resistance of the gas sensor. In addition, the quantity of silver paste used to affix the copper wire to the electrode's leg may impact the resistance of the gas sensor [64]

Table 4.1: Resistance values of the polymer-based gas sensor

Sample	**Resistance (Ω)**			
	1 Layer		2 Layer	
	Sample name	Resistance (Ω)	Sample name	Resistance (Ω)
Paste A	T1-1-S1	359.71 Ω	T1-2-S1	125.31 Ω
	T1-1-S2	357.14 Ω	T1-2-S2	120.92 Ω
	T1-1-S3	343.64 Ω	T1-2-S3	147.06 Ω
Paste B	T2-1-S1	591.72 Ω	T2-2-S1	432.90 Ω
	T2-1-S2	546.45 Ω	T2-2-S2	401.61 Ω
	T2-1-S3	526.32 Ω	T2-2-S3	452.49 Ω

4.4 Characterization of Sensing Layer using SEM and Raman

At magnifications of 1.0Kx, Figure 4.4 and Figure 4.5 depicts the morphology of the sensing layer of the gas sensor on the Kapton film for paste A and paste B respectively. The structure of the graphene may be seen to be nanoflakes typed similarly to those previously reported [64], [65]. The T1-1 (a) sample had more gaps between the graphene flakes than the T1-2 (b), T2-1 (c), and T2-2 (d) samples, which could be attributed to the lower amount of graphene dropped on the substrate. More gaps in the sensing layer allow more gas to flow into the sensing layer of the gas sensor, resulting in a stronger response and increased sensitivity [64].

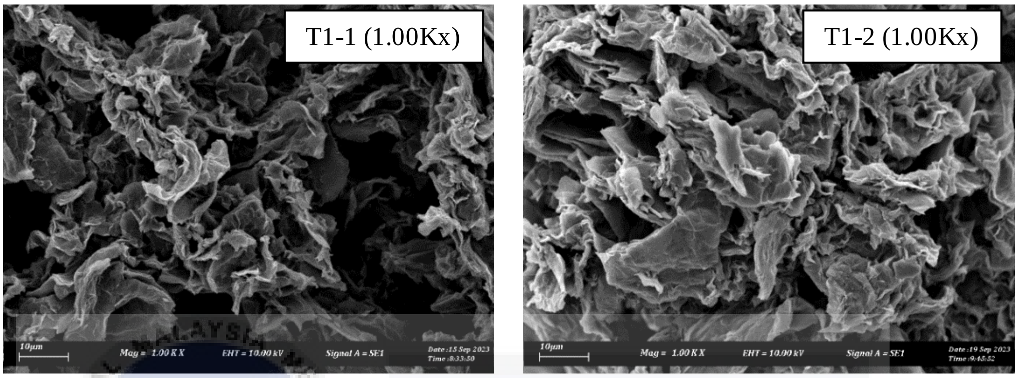

(a) (b)

Figure 4.4: Surface morphology of graphene using SEM for Paste A, (a) T1-1, and (b) T1-2

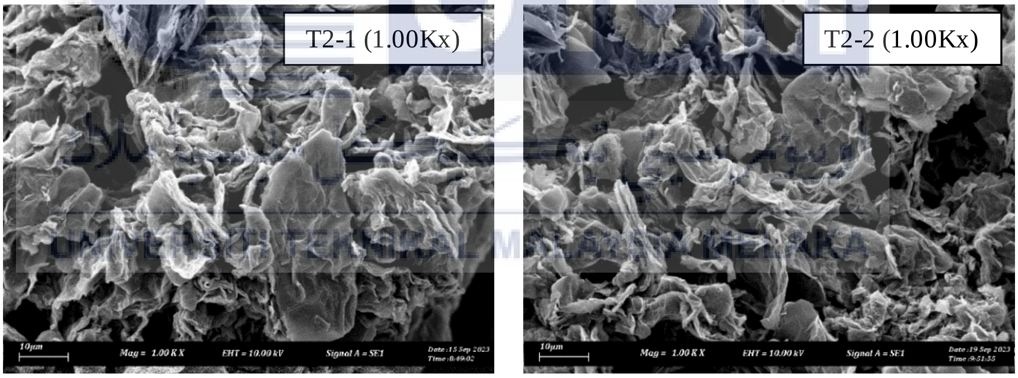

(a) (b)

Figure 4.5: Surface morphology of graphene using SEM for Paste B, (a) T2-1, and (b) T2-2

Figure 4.6 shows the result obtained from the Raman process using 1.00Kx of magnification. The result for T1-1L (D-1336.24 cm^{-1}, G-1571.31 cm^{-1}, 2D-2678.69 cm^{-1}), T1-2L (D-1339.55 cm^{-1}, G-1571.31 cm^{-1}, 2D-2682.01 cm^{-1}), T2-1L (D-1343.28 cm^{-1}, G-1571.31 cm^{-1}, 2D-2678.69 cm^{-1}), and T2-2L (D-1346.60 cm^{-1}, G-1578.36 cm^{-1}, 2D-2688.64 cm^{-1}). From the previous research, the peak appeared at (D-1350 cm^{-1}, G-1582 cm^{-1}, 2D-2700 cm^{-1}) [66]. Therefore, it verified the sensing material used was graphene as it is similar to other literature [66] [67].

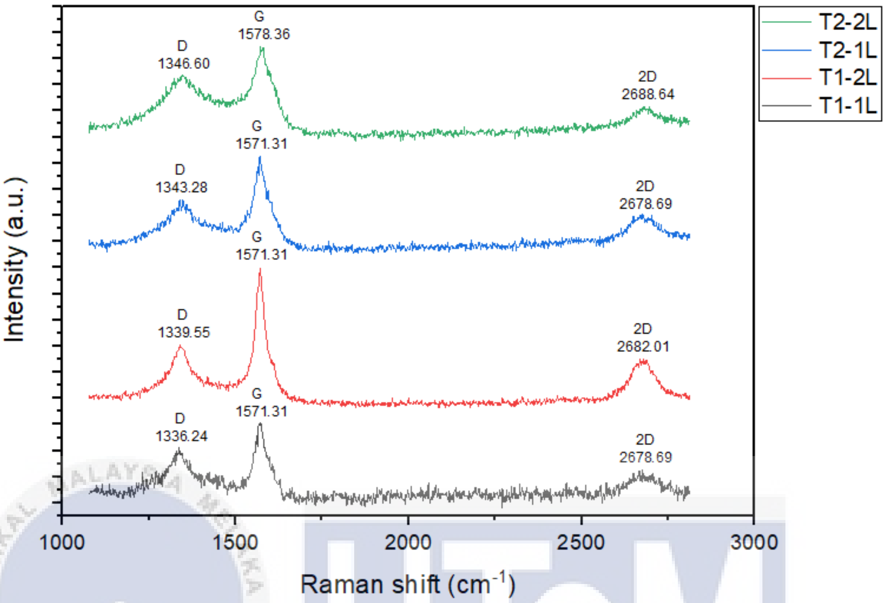

Figure 4.6: Raman spectra of graphene nanoflakes

4.5 Current Measurement Toward Acetone

This section details the key features of gas sensor performance, focusing on current measurement, response calculation, response time, recovery characteristics, and repeatability. It explains the underlying principles regulating recent changes in gas sensors, presents mathematical methods for response computation, and analyses response elements such as sensor materials and deposited technique. By examining these features in-depth, this subchapter intends to provide a thorough understanding of gas sensor behaviour, assisting researchers in optimizing sensor performance for a wide range of real-world applications.

4.5.1 Response and Response Time

Figure 4.7 presents the current measurement of polymer-based gas sensors toward acetone gas. The current measurement process started with exposing the sample to air for 15 minutes to ensure that it had stabilised at standard atmospheric pressure. It can be seen that all the gas sensors (T1-1, T1-2, T2-1, and T2-2) cannot reached the stability in air after 15 minutes. After that, the gas chamber's hose was connected to the acetone vapor for 30 minutes, the current value kept increasing during this period for all gas sensors, T1-1 (a), T1-2 (b), T2-1 (c), T2-2 (d) and it indicates the response of the sensor toward acetone similar with previous research which is p-type gas sensor [64], [65]. The glassware's hose was withdrawn from the gas chamber after 30 minutes, and the recovery time was recorded for 15 minutes. Among them, T1-1-S2(1), T2-1-S2(1), and T2-2-S3(1) showed saturated current when exposed to the acetone vapor, while other gas sensors were unable to saturate in 30 minutes.

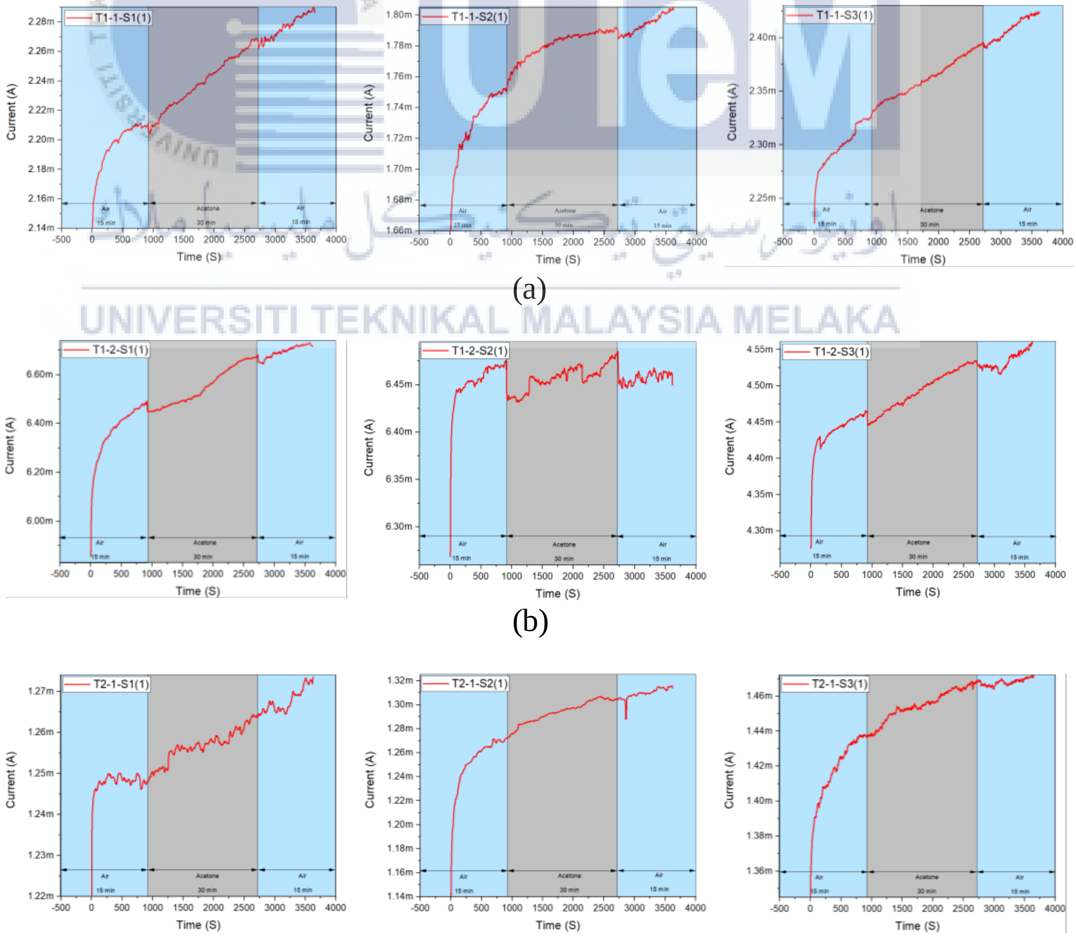

(a)

(b)

(c)

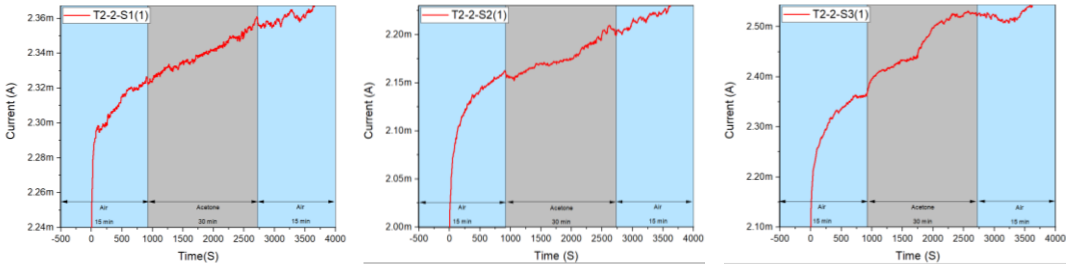

(d)

Figure 4.7: Current measurement of polymer gas sensor toward acetone, (a) T1-1, (b) T1-2, (c) T2-1, (d) T2-2

The polymer-based gas sensor's response, response time, and recovery to acetone are displayed in Table 4.2. The single layer for paste A is more significant than the double layer because the reaction is consistent within the range of 1.0211 to 1.0323. For paste A, 1.0697 (T1-2-S1(3)) is the greatest response value and 1.0040 (T1-1-S3(2)) is the lowest. In terms of response time, the double layer showed quicker response compared to the single layer within the range of 18 minutes to 28 minutes. The faster response time for paste A produced by T1-2-S2(3) (18 minutes) and the slower response time contributed by T1-1-S3(1) (29 minutes).

In contrast, paste B's double layer has greater significance than its single layer, with a consistent response within the range of 1.0123 to 1.0699. For paste B, 1.0703 (T2-1-S1(3)) is the greatest response value and 1.0041 (T2-1-S3(2)) is the lowest. Nonetheless, paste B's response was more substantial than paste A's, with a consistency of response ranging from 0.0100 to 1.0699. Therefore, the proposed binder (paste B) produced better response value compared to the paste A. As for the response time, the single layer shows a faster response time compared to a double layer which is between 3 minutes to 27 minutes. For paste B, the highest response time produced by T2-1-S3(2) (3 minutes), and the lowest response time produced by T2-2-S1(3) in 29 minutes. Lastly, for recovery characteristics, most of the sample were unable to recover after exposure to the acetone in 30 minutes. However, the result shows that paste A can recover better than paste B as the total sample that can recover is seven compared to three samples from paste B.

Table 4.2: Characteristics of polymer-based gas sensor toward acetone

Paste	Sample Name	Response	Response Time (s)	Recovery characteristic
Paste A	T1-1-S1(1)	1.0261	1580	No
	T1-1-S1(2)	1.0224	1737	No
	T1-1-S1(3)	1.0091	1659	No
	T1-1-S2(1)	1.0211	1336	No
	T1-1-S2(2)	1.0252	1667	No
	T1-1-S2(3)	1.0093	1537	No
	T1-1-S3(1)	1.0300	1746	No
	T1-1-S3(2)	1.0040	1667	Yes
	T1-1-S3(3)	1.0323	1729	No
	T1-2-S1(1)	1.0343	1474	No
	T1-2-S1(2)	1.0108	1554	Yes
	T1-2-S1(3)	1.0697	1737	Yes
	T1-2-S2(1)	1.0067	1607	Yes
	T1-2-S2(2)	1.0075	1484	Yes
	T1-2-S2(3)	1.0153	1108	Yes
	T1-2-S3(1)	1.0184	1545	No
	T1-2-S3(2)	1.0142	1518	No
	T1-2-S3(3)	1.0285	1536	Yes
Paste B	T2-1-S1(1)	1.0124	1667	No
	T2-1-S1(2)	1.0336	1563	No
	T2-1-S1(3)	1.0703	987	No
	T2-1-S2(1)	1.0266	1363	No
	T2-1-S2(2)	1.0100	1642	Yes
	T2-1-S2(3)	1.0123	1566	No
	T2-1-S3(1)	1.0212	1563	No
	T2-1-S3(2)	1.0041	166	No
	T2-1-S3(3)	1.0119	1632	No
	T2-2-S1(1)	1.0143	1606	No
	T2-2-S1(2)	1.0487	1764	No
	T2-2-S1(3)	1.0579	1772	No
	T2-2-S2(1)	1.0218	1371	No
	T2-2-S2(2)	1.0226	1318	No
	T2-2-S2(3)	1.0140	1521	Yes
	T2-2-S3(1)	1.0699	1396	No
	T2-2-S3(2)	1.0176	1082	No
	T2-2-S3(3)	1.0123	1414	Yes

4.5.2 Repeatability Properties

For a gas sensor to be reliable in practical applications, it must be repeatable. It relates to the sensor's capacity to generate repeatable, consistent readings under the same circumstances. This finding, which was made three times for every sample, points to a significant variation in the two pastes’ sensitivity to the target gases. Figure 4.8 shows the repeatability of the sensor response for three times exposure. It can be seen that all responses produced a similar pattern. T1-1-S1, T1-2-S1, T1-2-S2, T2-1-S2, T2-2-S1, and T2-2-S3 produced consistent patterns where the current response was produced in sequence from the first attempt to the third attempt of exposure. However, T1-1-S2, T1-1-S3, T1-2-S3, T2-1-S1, T2-1-S3, and T2-2-S2 did not produce a good pattern where the current measurement value overlapped between the first, second, and third attempts. As can be seen, T1-1-S3 showed a slightly different response among the three attempts but still in acceptable range of 2.10 mA - 3.0 mA.

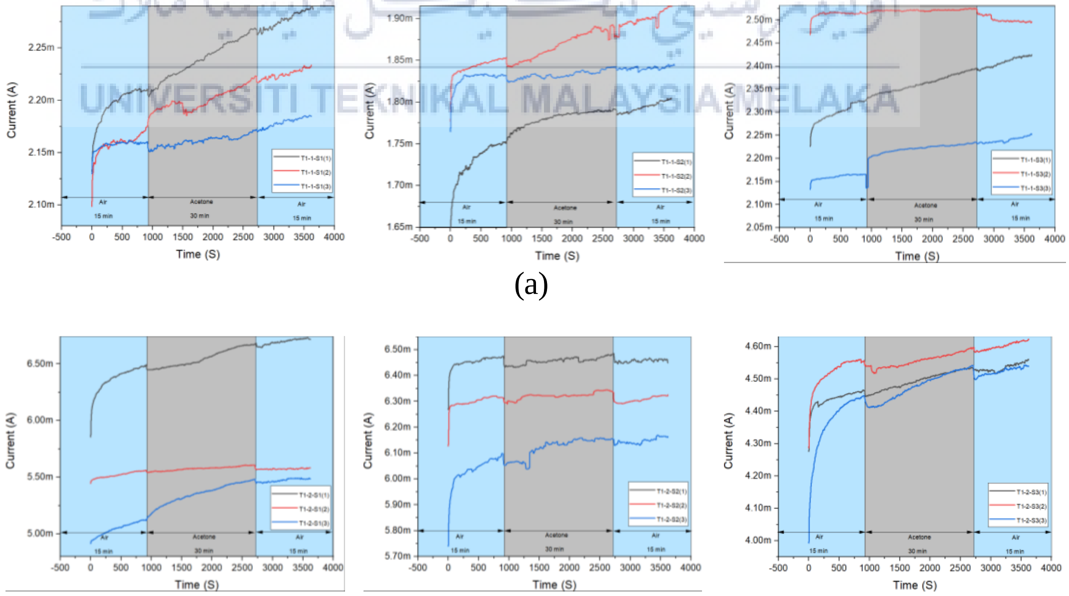

(a)

(b)

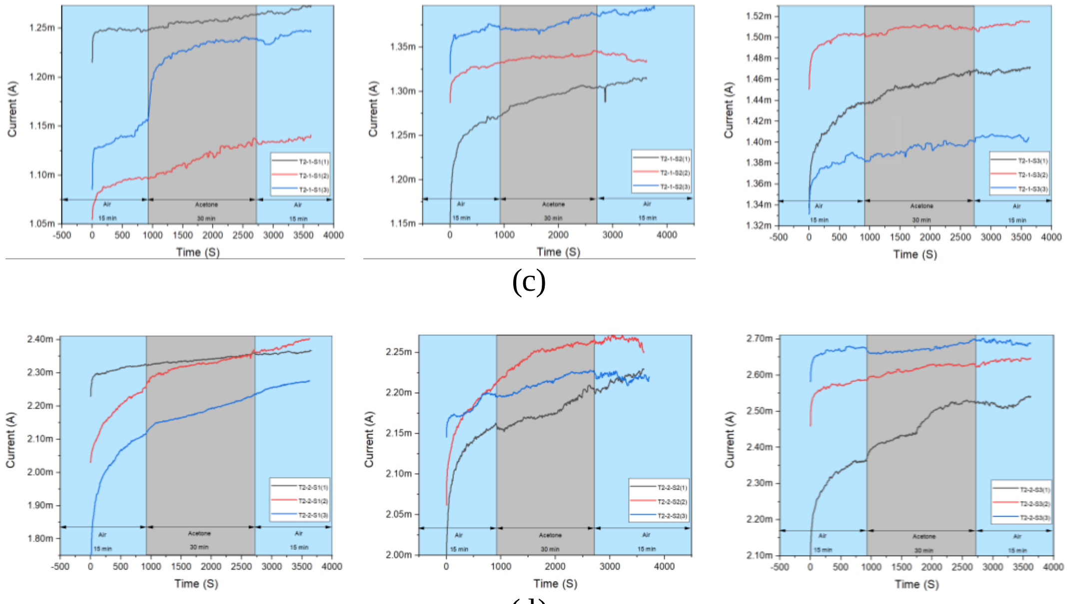

(c)

(d)

Figure 4.8: Repeatability of current measurement towards acetone, (a) Paste A- 1 layer, (b) Paste A- 2 layer, (c) Paste B- 1 layer, (d) Paste B- 2 layer

4.6 Current Measurement Toward Ethanol

This part discusses how gas sensors work, focusing on current measurement, responses, how quickly they react, how they recover, and how reliably they repeat their performance. It explains the basic rules behind the changes in current within gas sensors, introduces simple math methods for figuring out responses, and looks at elements like the materials used in the sensors and how they're made. By looking closely at these features, this section aims to help researchers understand the characteristics of gas sensor.

4.6.1 Response and Response Time

Figure 4.9 shows current measurement of polymer-based gas sensor to ethanol gas. Firstly, the sensor sample was left in the air for 15 minutes to make sure it was stable at regular air pressure. However, none of the samples (T1-1, T1-2, T2-1, and T2-2) became stable after 15 minutes. After that, the hose of the gas chamber was connected to ethanol vapor for 30 minutes, and the current values increased during this time for all sensors (T1-1, T1-2, T2-1, T2-2). This response pattern is similar to past research [64], [65] showing that this is a p-type gas sensor. After 30 minutes, the hose was removed from the gas chamber, and the time it took for the sensor to recover was recorded for 15 minutes. Some sensors (T1-1-S1(1), T2-2-S1(1), T2-2-S2(1), and T2-2-S3(1)) showed saturated current when exposed to the ethanol vapor, while other gas sensors were unable to saturate in 30 minutes.

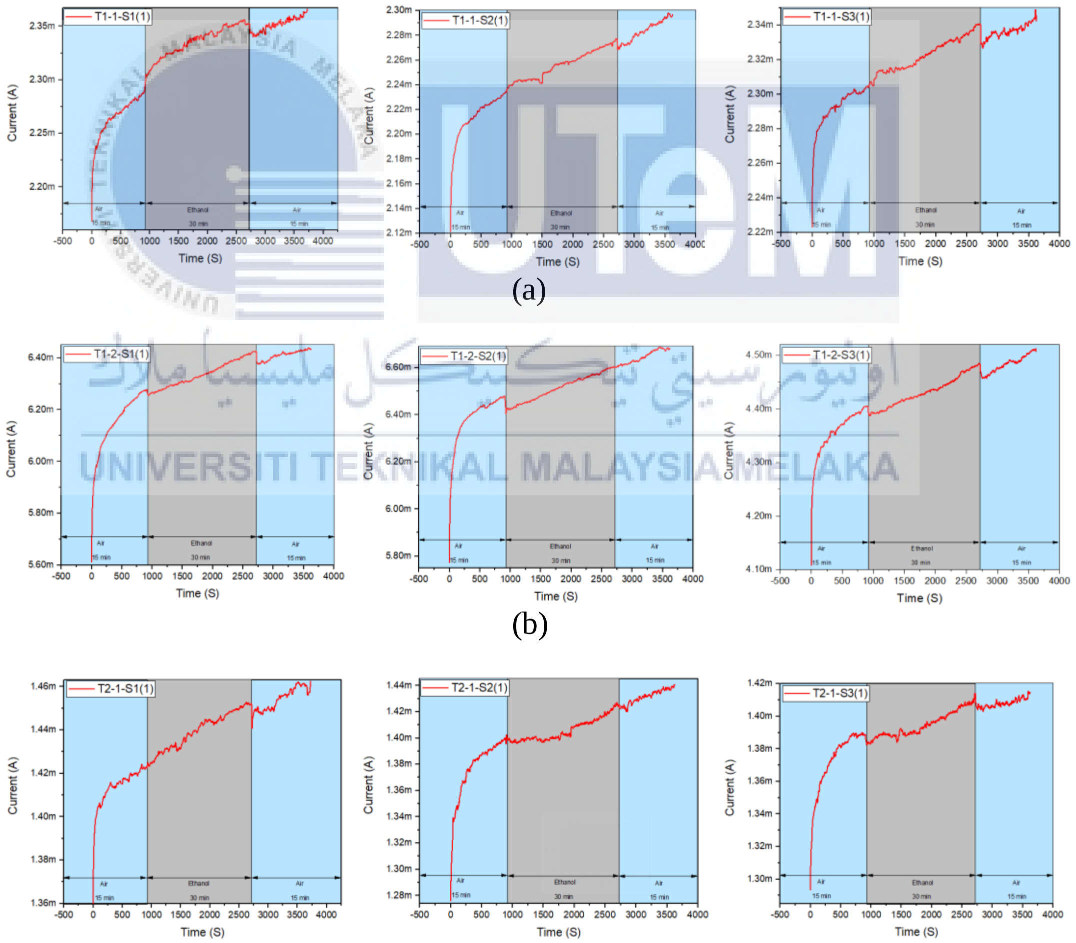

(a)

(b)

(c)

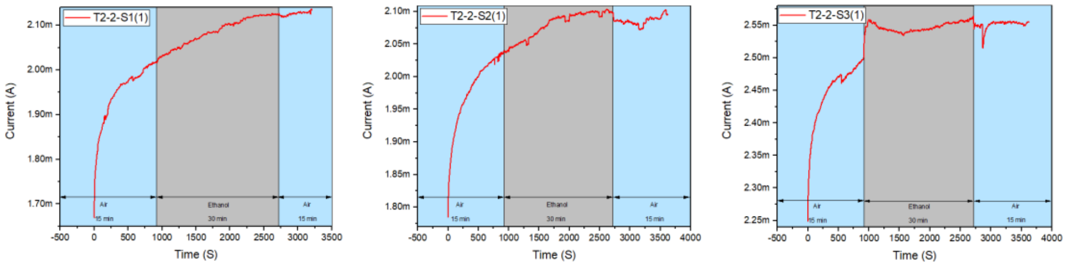

(d)

Figure 4.9: Current measurement of polymer-based gas sensor toward ethanol, (a) Paste A- 1 layer, (b) Paste A- 2 layer, (c) Paste B- 1 layer, (d) Paste B- 2 layer

Table 4.3 shows the characteristics of polymer-based gas sensor toward ethanol in term of response, response time and recovery time. In paste A, the single layer has a more noticeable reaction than the double layer because the response was consistent in between of 1.0110 and 1.0340. The highest response for paste A is 1.0340 (T1-1-S3(2)), and the lowest is 1.0099 (T1-2-S3(3)). The double layer in paste A responds faster, in between of 24 to 28 minutes. The quickest response is T1-1-S1(1) in 23 minutes, and the slowest is T1-1-S2(2) in 29 minutes.

On the other hand, paste B's double layer is more significant than the single layer, with a consistent response between 1.0207 and 1.0532. In paste B, the highest response is 1.1389 (T2-2-S2(2)), and the lowest is 1.0089 (T2-1-S3(2)). Paste B's response is overall more substantial than paste A's, ranging from 1.0143 to 1.0532. So, the suggested binder (paste B) performs better in terms of response compared to the paste A. In terms of response time, the single layer in paste B responded faster than the double layer, taking between 21 to 29 minutes. The highest response time is T2-2-S2(1) in 17 minutes, and the lowest is T2-1-S3(3) in 29 minutes. Regarding recovery, most samples couldn't recover after 30 minutes of exposure to acetone. However, both paste A and paste B show equal recovery, as the total samples that can recover were similar.

Table 4.3: Characteristic of polymer-based gas sensor toward ethanol

Paste	Sample Name	Response	Response Time (s)	Recovery characteristic
Paste A	T1-1-S1(1)	1.0285	1400	No
	T1-1-S1(2)	1.0115	1422	No
	T1-1-S1(3)	1.0110	1614	Yes
	T1-1-S2(1)	1.0185	1746	No
	T1-1-S2(2)	1.0267	1789	No
	T1-1-S2(3)	1.0300	1737	No
	T1-1-S3(1)	1.0155	1702	No
	T1-1-S3(2)	1.0340	1771	No
	T1-1-S3(3)	1.0046	1440	No
	T1-2-S1(1)	1.0235	1448	Yes
	T1-2-S1(2)	1.0076	1640	Yes
	T1-2-S1(3)	1.0109	1493	Yes
	T1-2-S2(1)	1.0278	1632	No
	T1-2-S2(2)	1.0333	1684	Yes
	T1-2-S2(3)	1.0068	1457	Yes
	T1-2-S3(1)	1.0209	1679	No
	T1-2-S3(2)	1.0137	1580	No
	T1-2-S3(3)	1.0099	1659	No
Paste B	T2-1-S1(1)	1.0207	1677	No
	T2-1-S1(2)	1.0098	1354	No
	T2-1-S1(3)	1.0364	1369	No
	T2-1-S2(1)	1.0179	1702	No
	T2-1-S2(2)	1.0166	1484	Yes
	T2-1-S2(3)	1.0151	1475	No
	T2-1-S3(1)	1.0143	1317	Yes
	T2-1-S3(2)	1.0089	1361	Yes
	T2-1-S3(3)	1.0224	1745	No
	T2-2-S1(1)	1.0532	1466	No
	T2-2-S1(2)	1.0428	1649	No
	T2-2-S1(3)	1.0096	1684	No
	T2-2-S2(1)	1.0299	1056	Yes
	T2-2-S2(2)	1.1389	1570	Yes
	T2-2-S2(3)	1.0283	1492	No
	T2-2-S3(1)	1.0249	1597	Yes
	T2-2-S3(2)	1.0253	1711	No
	T2-2-S3(3)	1.0207	1632	Yes

4.6.2 Repeatability properties

For a gas sensor to work well in real-life situations, it needs to give consistent results. This means it should provide the similar readings when exposed to the same circumstances. The current measurement was done three times for each sample. The results showed that the two pastes have different sensitivity to the target gases. Figure

4.10 illustrates how the sensor's response was consistent and followed the similar pattern. T1-2-S3 and T2-2-S1 consistently produced the same pattern of current response in sequence from the first attempt to the third attempt of exposure. However, T1-1-S1, T1-1-S2, T1-1-S3, T1-2-S1, T1-2-S2, T2-1-S1, T2-1-S2, T2-1-S3, T2-2-S2, and T2-2-S3 did not show a good pattern. The current measurement values were overlapped at first, second, and third attempts. It is noticeable that T2-1-S2 had a slightly different response among the three attempts but was still within an acceptable range.

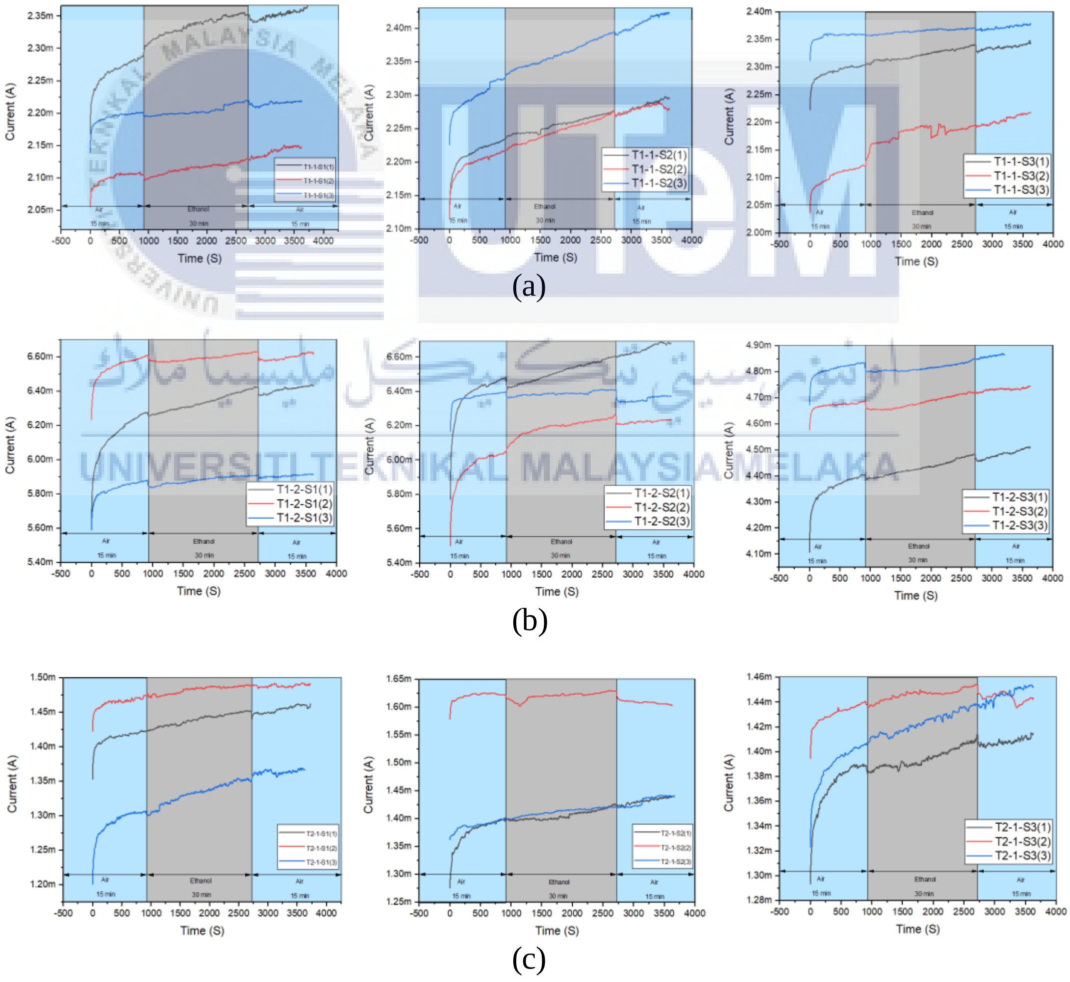

(a)

(b)

(c)

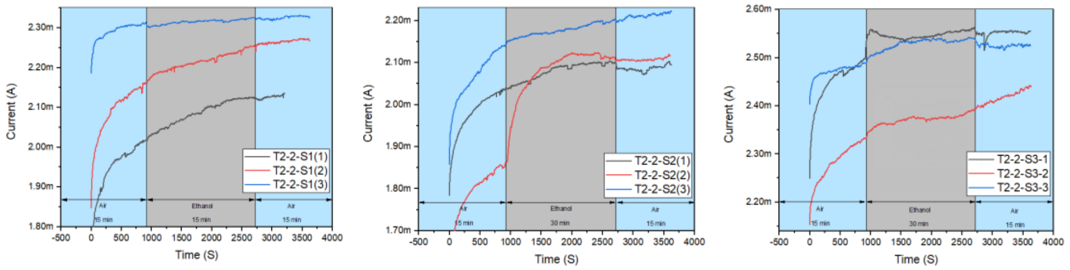

(d)

Figure 4.10: Repeatability of current measurement towards acetone, (a) Paste A- 1 layer, (b) Paste A- 2 layer, (c) Paste B- 1 layer, (d) Paste B- 2 layer

4.7 Comparison of Response for Acetone and Ethanol Gas Sensor

Table 4.4 compares the gas sensor in this study responds to acetone and ethanol with prior work. In the past research, the response to acetone was about 1.60%, but in this study, it was 1.07. Similarly, for ethanol, the prior research had a response of about 1.00, and this study showed a response of 1.05. These results suggest that the new binder proposed in this study could be an alternative for making gas sensors. Note that the response of previous research is in percent due to the different formulas used to calculate the response. However, to calculate using that formula, the current measurement must achieve in saturated condition. As for this finding, a different formula was used due to the sensor response was unable to saturate during gas exposure.

Table 4.4: Comparison of Response for Acetone and Ethanol Gas Sensor

Sensing Material	Binder	Technique	Gas	Response	References
Graphene	DI Water	Drop-casting	Acetone	1.60%	[64]
Graphene	Ethyl Cellulose	Doctor Blade	Ethanol	1.00	[68]
Graphene	Chitosan	Doctor Blade	Acetone	1.07	Current Work
Graphene	Chitosan	Doctor Blade	Ethanol	1.05	Current Work

CHAPTER 5

CONCLUSION AND FUTURE WORKS

5.1 Conclusion

The primary goal of this project is to develop a polymer-based gas sensor for volatile organic compounds and to analyse the characteristic of the sensor in terms of response, response time, and recovery time. The polymer-based gas sensor was successfully fabricated using the doctor blade technique on the Kapton film. All gas sensors responded well to the acetone and ethanol vapor. However, this sensor showed a good response toward acetone compared to the ethanol due to the highest response of 1.0697 in acetone, however it also has poor selectivity because the response were almost similar for all gas sensors. The linear I-V characteristic showed all the gas sensor values behaved electrically according to Ohm's law, which states that current (I) is inversely proportional to voltage (V). The resistance value of paste B is slightly higher than paste A due to the 2% chitosan used to fabricate the polymer solution B compared to the 1% chitosan in polymer solution A. The resistance value of the single layer for both pastes A and B showed a higher value compared to the double layer due to the twice annealed process and also it can affecting the amount of polymer that being evaporated. T1-2-S2 generated the lowest resistance, which is 120.92 Ω, whereas T2-1-S1 generated the highest resistance which is 591.72 Ω

In conclusion, the comparison of the gas sensor's response to the acetone and ethanol in this study highlights the promising performance of the novel binder. The response values obtained in this work, particularly 1.0703 (T2-1-S1(3)) for acetone and 1.0532 (T2-2-S1(1)) for ethanol, demonstrate its potential for fabricating effective gas sensors for VOC gases.

5.2 Future recommendations

Although the project is successful, there are few recommendations for improvement. The binder can be improved by doping the polymer with metal oxide, for example, zinc oxide, to enhance its properties. This can lead to improve the mechanical strength, electrical conductivity, and stability. Besides, the concentration of polymer also can affect the performance of the sensor. Therefore, reducing the polymer concentration to 0.5% during the preparation of the polymer solution process is suggested. As a result, it can produce a large gap between graphene nanoflakes and increase the sensor's response time.

5.3 Sustainable Development Goals (SDG)

The fabrication of polymer-based gas sensors is directly linked to SDG 3, which focuses on ensuring good health and well-being for all. The goal emphasizes the need to reduce the burden of diseases, including those resulting from environmental factors. In the case of gas sensors, the detection of volatile organic compounds (VOCs) such as ethanol and acetone contributes to public health. Prolonged exposure to these VOCs can lead to various health issues, including nausea, skin rashes, bronchitis, weariness, and even severe conditions like Parkinson's disease. By developing accurate and efficient gas sensors, the goal is to mitigate health risks associated with exposure to harmful gases, ultimately contributing to the improvement of public health and well-being.

Besides, SDG 12 focuses on responsible consumption and production patterns, aiming to ensure sustainable practices in the use of resources. In the context of polymer-based gas sensors, this goal is addressed through sustainable manufacturing processes and material choices. The selection of materials like graphene and chitosan, along with substrate choices such as Kapton, reflects a consideration for sustainable and eco-friendly options. Additionally, the emphasis on optimizing response, response time, and recovery time in gas sensor fabrication aligns with the goal of efficient resource utilization. The development of sensors with improved characteristics contributes to responsible production practices, reducing waste and optimizing resource efficiency.

In summary, the fabrication of polymer-based gas sensors is aligned with SDG 3 by addressing health concerns related to exposure to harmful gases. Simultaneously, it supports SDG 12 by promoting responsible consumption and production through sustainable material choices and efficient manufacturing processes. The integration of these goals ensures that technological advancements in gas sensor fabrication contribute to a healthier environment and a more sustainable future.

REFERENCES

[1] M. Masi, W. G. Nissim, C. Pandolfi, E. Azzarello, and S. Mancuso, “Modelling botanical biofiltration of indoor air streams contaminated by volatile organic compounds,” *J Hazard Mater*, vol. 422, p. 126875, Jan. 2022, doi: 10.1016/j.jhazmat.2021.126875.

[2] Minnesota Department of Health, “Volatile Organic Compounds in Your Home.”

[3] M. Souri, Y. Yamini, and H. S. Amoli, “The synergistic effect of Ce dopant/Cotton bio-template on the performance of the SnO2 gas sensor for the detection of Ethanol,” *Materials Science and Engineering: B*, vol. 294, p. 116501, Aug. 2023, doi: 10.1016/j.mseb.2023.116501.

[4] L. Wu *et al.*, “Ce-doped LaCoO $_3$ film as a promising gas sensor for ethanol,” *AIP Adv*, vol. 11, no. 5, p. 055305, May 2021, doi: 10.1063/5.0049923.

[5] T. Arakawa, K. Toma, and K. Mitsubayashi, “Bio-sniffer and sniff-cam,” in *Chemical, Gas, and Biosensors for Internet of Things and Related Applications*, Elsevier, 2019, pp. 271–288. doi: 10.1016/B978-0-12-815409-0.00019-X.

[6] T. CHLUDZIŃSKI, “System of breath collection and analysis for diseases detection,” *PRZEGLĄD ELEKTROTECHNICZNY*, vol. 1, no. 11, pp. 49–52, Nov. 2016, doi: 10.15199/48.2016.11.12.

[7] A. F. S. Abu-Hani, Y. E. Greish, S. T. Mahmoud, F. Awwad, and A. I. Ayesh, “Low-temperature and fast response H2S gas sensor using semiconducting chitosan film,” *Sens Actuators B Chem*, vol. 253, pp. 677–684, Dec. 2017, doi: 10.1016/j.snb.2017.06.103.

[8] J. R. F. Foronda, L. G. Aryaswara, G. N. C. Santos, S. N. V. Raghu, and M. A. Muflikhun, “Broad-class volatile organic compounds (VOCs) detection via polyaniline/zinc oxide (PANI/ZnO) composite materials as gas sensor application,” *Heliyon*, vol. 9, no. 2, p. e13544, Feb. 2023, doi: 10.1016/j.heliyon.2023.e13544.

[9] S. P. Bharath, K. V. Bangera, and G. K. Shivakumar, “Synthesis and characterization of Cu1-xZnxO composite thin films for sensor application,” *Ceram Int*, vol. 45, no. 10, pp. 12691–12699, Jul. 2019, doi: 10.1016/j.ceramint.2019.03.117.

[10] B. Bouricha, R. Souissi, N. Bouguila, and A. Labidi, “A real-time sharp selectivity with In2S3 gas sensor using a nonlinear dynamic response for

VOCs," *Measurement*, vol. 185, p. 110070, Nov. 2021, doi: 10.1016/j.measurement.2021.110070.

[11] M. Gupta, N. Athirah, and H. Fahmi Hawari, "Graphene derivative coated QCM-based gas sensor for volatile organic compound (VOC) detection at room temperature," *Indonesian Journal of Electrical Engineering and Computer Science*, vol. 18, no. 3, p. 1279, Jun. 2020, doi: 10.11591/ijeecs.v18.i3.pp1279-1286.

[12] N. C. Wijayanti, R. D. Cahyaningrum, and Harsojo, "Study of Thin Film Cu Nanowire and Reduced Graphene Oxide as A Gas Sensor," *J Phys Conf Ser*, vol. 1494, no. 1, p. 012036, Mar. 2020, doi: 10.1088/1742-6596/1494/1/012036.

[13] C. Li, P. G. Choi, K. Kim, and Y. Masuda, "High performance acetone gas sensor based on ultrathin porous NiO nanosheet," *Sens Actuators B Chem*, vol. 367, p. 132143, Sep. 2022, doi: 10.1016/j.snb.2022.132143.

[14] Y. Chen *et al.*, "Highly sensitive and selective acetone gas sensors based on modified ZnO nanomaterials," *Mater Sci Semicond Process*, vol. 148, p. 106807, Sep. 2022, doi: 10.1016/j.mssp.2022.106807.

[15] M. Jali, "Detection of acetone as a potential non-invasive diagnosis tool for diabetes patients," *PRZEGLĄD ELEKTROTECHNICZNY*, vol. 1, no. 5, pp. 73–77, May 2022, doi: 10.15199/48.2022.05.13.

[16] L. Lyu *et al.*, “A novel CeO2 Hollow-Shell sensor constructed for high sensitivity of acetone gas detection,” *Appl Surf Sci*, vol. 571, p. 151337, Jan. 2022, doi: 10.1016/j.apsusc.2021.151337.

[17] H. Park *et al.*, “Flexible and disposable paper-based gas sensor using reduced graphene oxide/chitosan composite,” *J Mater Sci Technol*, vol. 101, pp. 165–172, Feb. 2022, doi: 10.1016/j.jmst.2021.06.018.

[18] Q. Jiang *et al.*, “Ultra-responsive and selective ethanol and acetone sensor based on Ce-doped Co3O4 microspheres assembled by submicron spheres with multilayer core-shell structure,” *Colloids Surf A Physicochem Eng Asp*, vol. 666, p. 131301, Jun. 2023, doi: 10.1016/j.colsurfa.2023.131301.

[19] H. J. Cheon, S. Y. Shin, V. Van Tran, B. Park, H. Yoon, and M. Chang, “Preparation of conjugated polymer/reduced graphene oxide nanocomposites for high-performance volatile organic compound sensors,” *Chemical Engineering Journal*, vol. 425, p. 131424, Dec. 2021, doi: 10.1016/j.cej.2021.131424.

[20] M. Ghazi, S. Janfaza, H. Tahmooressi, N. Tasnim, and M. Hoorfar, “Selective detection of VOCs using microfluidic gas sensor with embedded cylindrical microfeatures coated with graphene oxide,” *J Hazard Mater*, vol. 424, p. 127566, Feb. 2022, doi: 10.1016/j.jhazmat.2021.127566.

[21] P. M. Biranje *et al.*, “Ultra-Fast Detection and Monitoring of Cancerous Volatile Organic Compounds in Environment Using Graphene Oxide Modified

CNT Aerogel Hybrid Gas Sensor," *SSRN Electronic Journal*, 2022, doi: 10.2139/ssrn.4147606.

[22] R. Kumar, H. Rahman, S. Ranwa, A. Kumar, and G. Kumar, "Development of cost effective metal oxide semiconductor based gas sensor over flexible chitosan/PVP blended polymeric substrate," *Carbohydr Polym*, vol. 239, p. 116213, Jul. 2020, doi: 10.1016/j.carbpol.2020.116213.

[23] D. Zhang, Z. Wu, and X. Zong, "Flexible and highly sensitive H2S gas sensor based on in-situ polymerized SnO2/rGO/PANI ternary nanocomposite with application in halitosis diagnosis," *Sens Actuators B Chem*, vol. 289, pp. 32–41, Jun. 2019, doi: 10.1016/j.snb.2019.03.055.

[24] M. O. Diniz, A. F. Golin, M. C. Santos, R. F. Bianchi, and E. M. Guerra, "Improving performance of polymer-based ammonia gas sensor using POMA/V2O5 hybrid films," *Org Electron*, vol. 67, pp. 215–221, Apr. 2019, doi: 10.1016/j.orgel.2019.01.039.

[25] M. Ramezannezhad, M. M. Akram, A. Nikfarjam, and S. Ehyaei, "Polymeric micro gas preconcentrators based on graphene oxide and carbon nanopowder adsorbents for gas detection application," *Micro and Nano Engineering*, vol. 15, p. 100139, Jun. 2022, doi: 10.1016/j.mne.2022.100139.

[26] M. Moschogiannaki, E. Gagaoudakis, G. Kiriakidis, and V. Binas, "Effect of the deposition method and substrate on an ultra-stable CoV2O6 hydrogen gas sensor, operating at room temperature," *Microelectron Eng*, vol. 262, p. 111819, Jun. 2022, doi: 10.1016/j.mee.2022.111819.

[27] Y. Liu *et al.*, “Controllable fabrication of oriented micro/nanowire arrays of dibenzo-tetrathiafulvalene by a multiple drop-casting method,” *Nanoscale*, vol. 6, no. 3, pp. 1323–1328, 2014, doi: 10.1039/C3NR05680E.

[28] S. Riera-Galindo, A. Tamayo, and M. Mas-Torrent, “Role of Polymorphism and Thin-Film Morphology in Organic Semiconductors Processed by Solution Shearing,” *ACS Omega*, vol. 3, no. 2, pp. 2329–2339, Feb. 2018, doi: 10.1021/acsomega.8b00043.

[29] V. S. Bhati *et al.*, “Improved Sensitivity with Low Limit of Detection of a Hydrogen Gas Sensor Based on rGO-Loaded Ni-Doped ZnO Nanostructures,” *ACS Appl Mater Interfaces*, vol. 10, no. 13, pp. 11116–11124, Apr. 2018, doi: 10.1021/acsami.7b17877.

[30] R. D. Deegan, O. Bakajin, T. F. Dupont, G. Huber, S. R. Nagel, and T. A. Witten, “Contact line deposits in an evaporating drop,” *Phys Rev E*, vol. 62, no. 1, pp. 756–765, Jul. 2000, doi: 10.1103/PhysRevE.62.756.

[31] A. Agrawal, S. A. Siddiqui, A. Soni, K. Khandelwal, and G. D. Sharma, “Performance analysis of TiO2 based dye sensitized solar cell prepared by screen printing and doctor blade deposition techniques,” *Solar Energy*, vol. 226, pp. 9–19, Sep. 2021, doi: 10.1016/j.solener.2021.08.001.

[32] M. R. Somalu, A. Muchtar, W. R. W. Daud, and N. P. Brandon, “Screen-printing inks for the fabrication of solid oxide fuel cell films: A review,” *Renewable and Sustainable Energy Reviews*, vol. 75, pp. 426–439, Aug. 2017, doi: 10.1016/j.rser.2016.11.008.

[33] D. Boonthum *et al.*, “Screen-Printing of Functionalized MWCNT-PEDOT:PSS Based Solutions on Bendable Substrate for Ammonia Gas Sensing,” *Micromachines (Basel)*, vol. 13, no. 3, p. 462, Mar. 2022, doi: 10.3390/mi13030462.

[34] N. L. Myadam, D. Y. Nadargi, J. D. Nadargi, and M. G. Chaskar, “Cu/SnO2 xerogels: a novel epoxide derived nanomaterial as formaldehyde gas sensor,” *J Solgel Sci Technol*, vol. 96, no. 1, pp. 56–66, Oct. 2020, doi: 10.1007/s10971-020-05377-x.

[35] P. Nagarjuna, K. Narayanaswamy, T. Swetha, G. H. Rao, S. P. Singh, and G. D. Sharma, “CH3NH3PbI3 Perovskite Sensitized Solar Cells Using a D-A Copolymer as Hole Transport Material,” *Electrochim Acta*, vol. 151, pp. 21–26, Jan. 2015, doi: 10.1016/j.electacta.2014.11.003.

[36] I. S. Mohamad, S. S. Ismail, M. N. Norizan, S. A. Z. Murad, and M. M. A. Abdullah, “ZnO Photoanode Effect on the Efficiency Performance of Organic Based Dye Sensitized Solar Cell,” *IOP Conf Ser Mater Sci Eng*, vol. 209, p. 012028, Jun. 2017, doi: 10.1088/1757-899X/209/1/012028.

[37] H. A. M. Mustafa and D. A. Jameel, “Modeling and the main stages of spin coating process: A review,” *Journal of Applied Science and Technology Trends*, vol. 2, no. 03, pp. 91–95, Aug. 2021, doi: 10.38094/jastt203109.

[38] R. Das and A. Chanda, “Fabrication and Properties of Spin-Coated Polymer Films,” in *Nano-size Polymers*, Cham: Springer International Publishing, 2016, pp. 283–306. doi: 10.1007/978-3-319-39715-3_10.

[39] A. A.-S. H. A. Bekir Sami Yilbas, *Self-Cleaning of Surfaces and Water Droplet Mobility*. Elsevier, 2019. doi: 10.1016/C2017-0-02187-0.

[40] W. Zhang, G. Chen, H. Wang, P. Chen, B. Zhang, and D. Zhang, “High-performance ammonia gas sensor based on bimetallic oxide Zn2SnO4 decorated with reduced graphene oxide,” *Journal of Materials Science: Materials in Electronics*, vol. 32, no. 15, pp. 20139–20148, Aug. 2021, doi: 10.1007/s10854-021-06483-4.

[41] M. V. Nikolic, V. Milovanovic, Z. Z. Vasiljevic, and Z. Stamenkovic, “Semiconductor Gas Sensors: Materials, Technology, Design, and Application,” *Sensors*, vol. 20, no. 22, p. 6694, Nov. 2020, doi: 10.3390/s20226694.

[42] A. Mirzaei, B. Hashemi, and K. Janghorban, “α-Fe2O3 based nanomaterials as gas sensors,” *Journal of Materials Science: Materials in Electronics*, vol. 27, no. 4, pp. 3109–3144, Apr. 2016, doi: 10.1007/s10854-015-4200-z.

[43] C. Wei *et al.*, “A Three-Dimensionally Structured Electrocatalyst: Cobalt-Embedded Nitrogen-Doped Carbon Nanotubes/Nitrogen-Doped Reduced Graphene Oxide Hybrid for Efficient Oxygen Reduction,” *Chemistry - A European Journal*, vol. 23, no. 3, pp. 637–643, Jan. 2017, doi: 10.1002/chem.201604113.

[44] J. T. Robinson, F. K. Perkins, E. S. Snow, Z. Wei, and P. E. Sheehan, “Reduced Graphene Oxide Molecular Sensors,” *Nano Lett*, vol. 8, no. 10, pp. 3137–3140, Oct. 2008, doi: 10.1021/nl8013007.

[45] J. Feng, Y. Ye, M. Xiao, G. Wu, and Y. Ke, “Synthetic routes of the reduced graphene oxide,” *Chemical Papers*, vol. 74, no. 11, pp. 3767–3783, Nov. 2020, doi: 10.1007/s11696-020-01196-0.

[46] K. Erickson, R. Erni, Z. Lee, N. Alem, W. Gannett, and A. Zettl, “Determination of the Local Chemical Structure of Graphene Oxide and Reduced Graphene Oxide,” *Advanced Materials*, vol. 22, no. 40, pp. 4467–4472, Oct. 2010, doi: 10.1002/adma.201000732.

[47] Y. Wang, W. Wang, R. Xu, M. Zhu, and D. Yu, “Flexible, durable and thermal conducting thiol-modified rGO-WPU/cotton fabric for robust electromagnetic interference shielding,” *Chemical Engineering Journal*, vol. 360, pp. 817–828, Mar. 2019, doi: 10.1016/j.cej.2018.12.045.

[48] M. A. Farea *et al.*, “Impact of reduced graphene oxide on the sensing performance of Poly (3, 4–ethylenedioxythiophene) towards highly sensitive and selective CO sensor: A comprehensive study,” *Synth Met*, vol. 291, p. 117166, Dec. 2022, doi: 10.1016/j.synthmet.2022.117166.

[49] J. Kong *et al.*, “Nanotube Molecular Wires as Chemical Sensors,” *Science (1979)*, vol. 287, no. 5453, pp. 622–625, Jan. 2000, doi: 10.1126/science.287.5453.622.

[50] P. G. Collins, K. Bradley, M. Ishigami, and A. Zettl, “Extreme Oxygen Sensitivity of Electronic Properties of Carbon Nanotubes,” *Science (1979)*, vol. 287, no. 5459, pp. 1801–1804, Mar. 2000, doi: 10.1126/science.287.5459.1801.

[51] M. Mittal and A. Kumar, "Carbon nanotube (CNT) gas sensors for emissions from fossil fuel burning," *Sens Actuators B Chem*, vol. 203, pp. 349–362, Nov. 2014, doi: 10.1016/j.snb.2014.05.080.

[52] J. Dai *et al.*, "Printed gas sensors," *Chem Soc Rev*, vol. 49, no. 6, pp. 1756–1789, 2020, doi: 10.1039/C9CS00459A.

[53] S. Mao, G. Lu, and J. Chen, "Nanocarbon-based gas sensors: progress and challenges," *J Mater Chem A Mater*, vol. 2, no. 16, p. 5573, 2014, doi: 10.1039/c3ta13823b.

[54] Y. Wang and J. T. W. Yeow, "A Review of Carbon Nanotubes-Based Gas Sensors," *J Sens*, vol. 2009, pp. 1–24, 2009, doi: 10.1155/2009/493904.

[55] Y. M. Wong, W. P. Kang, J. L. Davidson, A. Wisitsora-at, and K. L. Soh, "A novel microelectronic gas sensor utilizing carbon nanotubes for hydrogen gas detection," *Sens Actuators B Chem*, vol. 93, no. 1–3, pp. 327–332, Aug. 2003, doi: 10.1016/S0925-4005(03)00213-2.

[56] S. Sharma, S. Hussain, S. Singh, and S. S. Islam, "MWCNT-conducting polymer composite based ammonia gas sensors: A new approach for complete recovery process," *Sens Actuators B Chem*, vol. 194, pp. 213–219, Apr. 2014, doi: 10.1016/j.snb.2013.12.050.

[57] S. Tang, W. Chen, H. Zhang, Z. Song, Y. Li, and Y. Wang, "The Functionalized Single-Walled Carbon Nanotubes Gas Sensor With Pd Nanoparticles for

Hydrogen Detection in the High-Voltage Transformers," *Front Chem*, vol. 8, Apr. 2020, doi: 10.3389/fchem.2020.00174.

[58] O. S. Kwon *et al.*, "Multidimensional Conducting Polymer Nanotubes for Ultrasensitive Chemical Nerve Agent Sensing," *Nano Lett*, vol. 12, no. 6, pp. 2797–2802, Jun. 2012, doi: 10.1021/nl204587t.

[59] A. Verma, R. Gupta, A. S. Verma, and T. Kumar, "A review of composite conducting polymer-based sensors for detection of industrial waste gases," *Sensors and Actuators Reports*, vol. 5, p. 100143, Jun. 2023, doi: 10.1016/j.snr.2023.100143.

[60] Y. C. Wong, B. C. Ang, A. S. M. A. Haseeb, A. A. Baharuddin, and Y. H. Wong, "Review—Conducting Polymers as Chemiresistive Gas Sensing Materials: A Review," *J Electrochem Soc*, vol. 167, no. 3, p. 037503, Sep. 2020, doi: 10.1149/2.0032003JES.

[61] M. Tonezzer and L. Van Duy, "Gas Sensors," in *Encyclopedia of Sensors and Biosensors*, Elsevier, 2023, pp. 185–208. doi: 10.1016/B978-0-12-822548-6.00113-8.

[62] W. Chen, Q. Zhou, F. Wan, and T. Gao, "Gas Sensing Properties and Mechanism of Nano-SnO $_2$ -Based Sensor for Hydrogen and Carbon Monoxide," *J Nanomater*, vol. 2012, pp. 1–9, 2012, doi: 10.1155/2012/612420.

[63] N. L. Lukman Hekiem *et al.*, "Effect of chitosan dissolved in different acetic acid concentration towards VOC sensing performance of quartz crystal

microbalance overlay with chitosan," *Mater Lett*, vol. 291, p. 129524, May 2021, doi: 10.1016/j.matlet.2021.129524.

[64] S. Chachuli, "Investigation of Graphene Gas Sensor at Different Substrates for Acetone Detection," *PRZEGLĄD ELEKTROTECHNICZNY*, vol. 1, no. 3, pp. 291–295, Mar. 2023, doi: 10.15199/48.2023.03.51.

[65] S. Amaniah Mohd Chachuli, M. Luqman Hakkim Noor, O. Coban, N. Hazahsha Shamsudin, and M. Idzdihar Idris, "Characteristic of graphene-based thick film gas sensor for ethanol and acetone vapor detection at room temperature," *Indonesian Journal of Electrical Engineering and Computer Science*, vol. 32, no. 3, p. 1384, Dec. 2023, doi: 10.11591/ijeecs.v32.i3.pp1384-1391.

[66] L. M. Malard, M. A. Pimenta, G. Dresselhaus, and M. S. Dresselhaus, "Raman spectroscopy in graphene," *Phys Rep*, vol. 473, no. 5–6, pp. 51–87, Apr. 2009, doi: 10.1016/j.physrep.2009.02.003.

[67] R. S. Sharbidre, C. J. Lee, S.-G. Hong, J.-K. Ryu, and T. N. Kim, "Comparison of Existing Methods to Identify the Number of Graphene Layers," *Korean Journal of Materials Research*, vol. 26, no. 12, pp. 704–708, Dec. 2016, doi: 10.3740/MRSK.2016.26.12.704.

[68] Amaniah Mohd Chachuli S, Luqman Hakkim Noor M, Omer Coban, and N.H. Shamsudin, "Thick Film Graphene Gas Sensor using Doctor Blade for Ethanol Sensing".

APPENDICES

APPENDIX A

Sample name:

T1 – 1 – S1 (1)

T1

Type of paste:
T1 = Paste A
T2 = Paste B

1

Number of layer:
1 = 1 layer
2 = 2 layer

S1

Number of sample:
S1 = Sample 1
S2 = Sample 2
S3 = Sample 3

(1)

Number of current measurement:
(1) = first expose
(2) = second expose
(3) = third expose

APPENDIX B

I-V measurement for paste A- 1 layer at 2 V, 3 V and 4 V

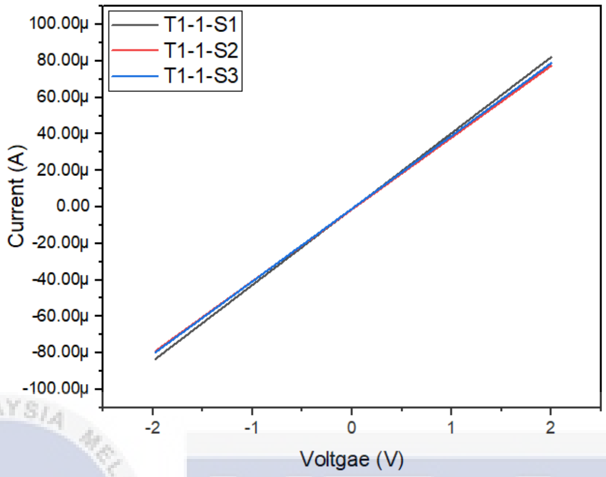

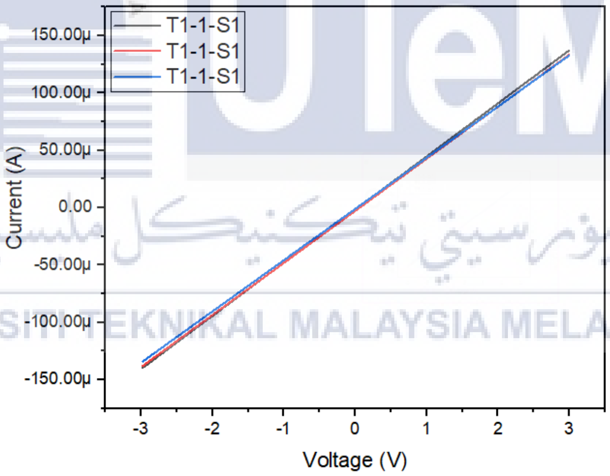

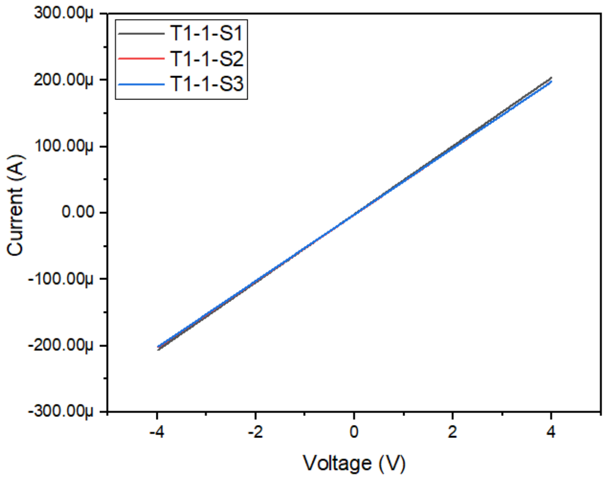

APPENDIX C

I-V measurement for paste A- 2 layer at 2 V, 3 V and 4 V

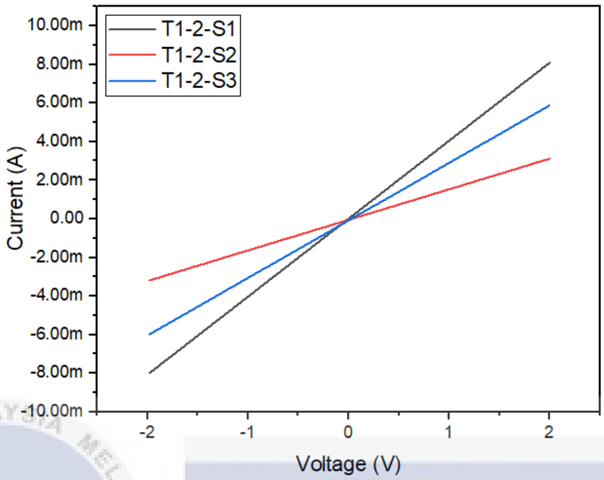

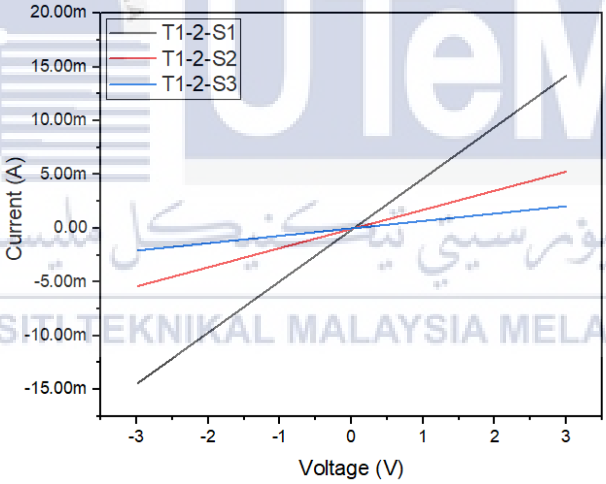

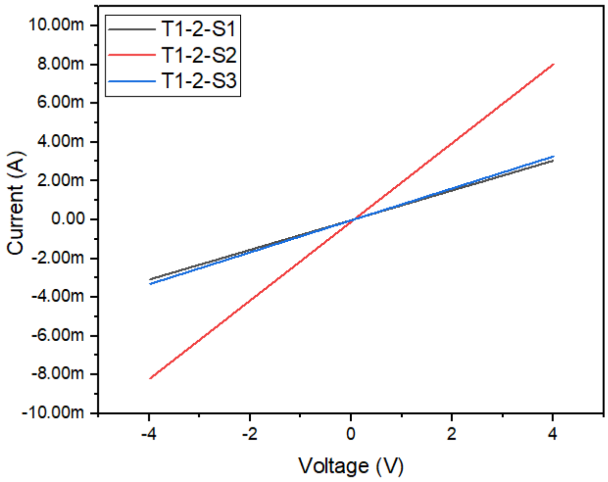

APPENDIX D

I-V measurement for paste B- 1 layer at 2V, 3V and 4V

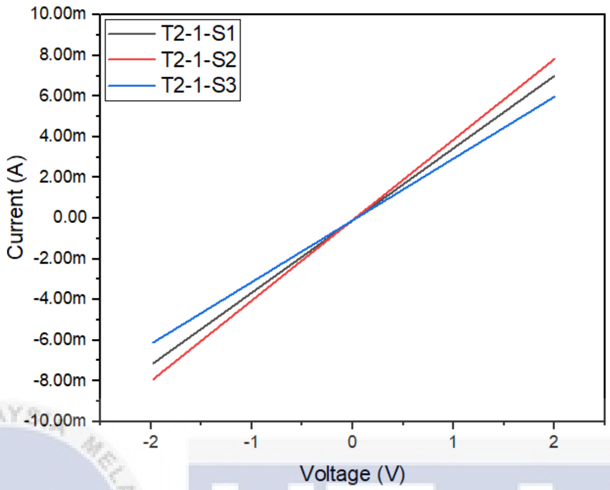

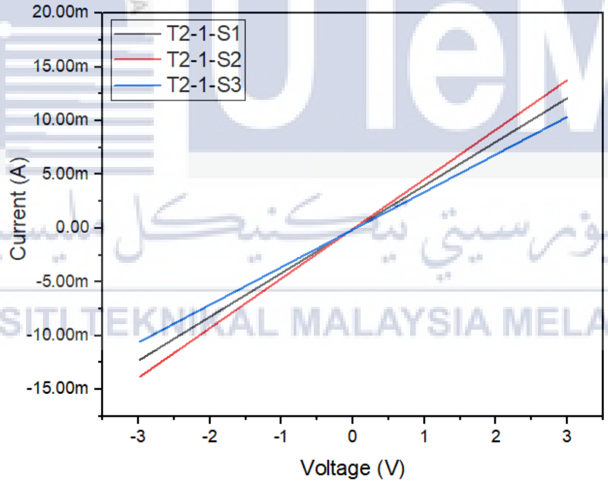

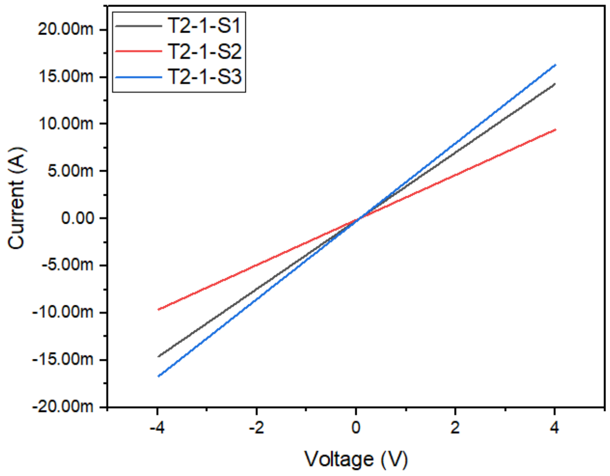

APPENDIX E

I-V measurement for paste B- 2 layer at 2V, 3V, 4V